Development of a Computational Model of Respiratory Mechanics in Mechanical Ventilation

Master thesis report

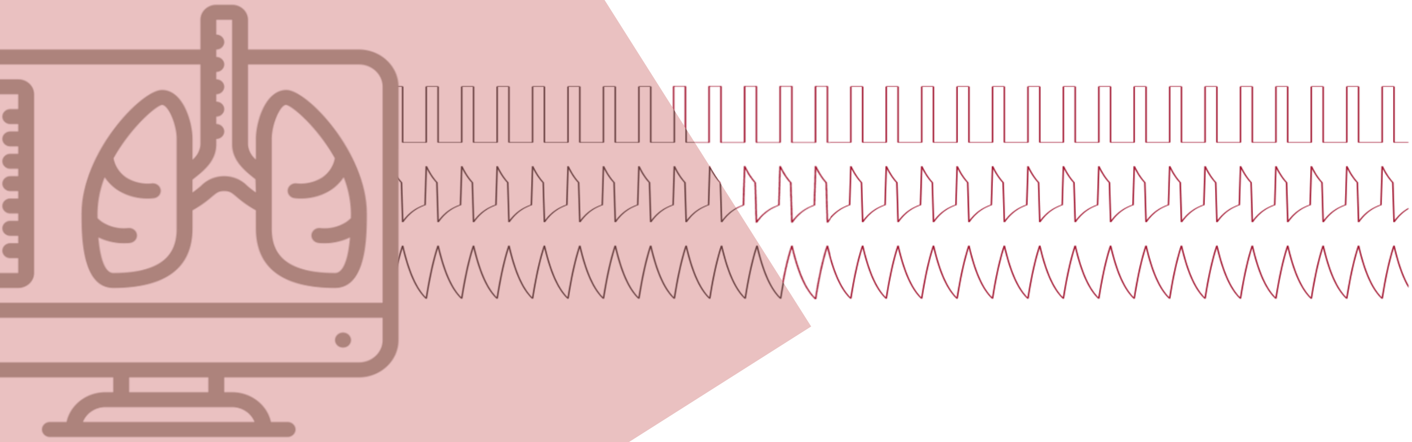

A. Mousa
Technical Medicine
September 2019 - August 2020

DEVELOPMENT OF A COMPUTATIONAL MODEL OF RESPIRATORY MECHANICS IN MECHANICAL VENTILATION

A thesis submitted to the Delft University of Technology, the Erasmus University
Rotterdam and the Leiden University in partial fulfillment
of the requirements for the degree of

Master of Science in Technical Medicine

by

Amne Mousa

at the Delft University of Technology, to be defended publicly on
Thursday August 27st, 2020 at 14.30h.

Student number:	4379314
Master programme:	Technical Medicine
Master track:	Sensing and Stimulation

University:	Technical University Delft	Faculty of Mechanical, Maritime and Materials Engineering (3mE)
	Leiden University	Leiden University Medical Centre (LUMC)
	Erasmus University Rotterdam	Erasmus Medical Centre (Erasmus MC)

Graduation committee: Prof. Dr. Ir. J. Harlaar
Dr. Ir. K. Batselier
Prof. Dr. E. de Jonge

Supervisors: Dr. Ir. K. Batselier
Drs. A. Schoe
Drs. P. Somhorst

PREFACE

All models are wrong, but some are useful - George E. P. Box

Breathing is something that most healthy individuals do not give a second thought; it is almost effortless and regulated automatically. There are, however, several diseases that cause breathing problems and in some cases lead to respiratory failure; the individual is not able to breathe without the assistance of a mechanical ventilator. Mechanical ventilation does not come without risks. The aim of mechanical ventilation is to provide gas exchange but limit ventilation induced lung injury, also known as VILI. The effects of mechanical ventilation on the lung and actually the entire body are complex. Understanding lung pathology and mechanical ventilation is of utmost importance for safe and effective treatment. Computational lung models have been widely used to understand and gain new insights about (mechanical) ventilation and to explore new techniques or algorithms for mechanical ventilation. Lung models allow for so called *in silico* studies; the use of simulation to study and answer research questions. Unfortunately, the lung models used in literature are not open source and thus do not allow for us to explore these models and perform in silico studies. This thesis describes the development and use of linear models of respiratory mechanics during mechanical ventilation. The aim of the model is firstly to educate the physicians and nurses of the Intensive Care Unit (ICU) in the Leiden University Medical Centre (LUMC). By usage of the models to visualize the effects of mechanical ventilation we hope to better educate the team of the ICU about the relation between respiratory mechanics and mechanical ventilation. Second, the model will be used to perform in silico studies. Many aspects of mechanical ventilation and interaction with the lung tissue are yet unknown. We hope to better understand this interaction to further optimise mechanical ventilation for better patient outcomes.

Chapter 1 gives an introduction to the thesis by discussing the most important aspects of mechanical ventilation at the ICU and mathematical modelling. Chapter 2 is a short overview of the most important respiratory mechanics relevant to the development of the models in this thesis. Of course, the respiratory mechanics are far more complicated than discussed in this thesis. Modelling in this thesis is split in to two parts: system identification (chapters 3 - 6) and simulation (chapter 7). Chapter 3 lays out the principles of system identification. System identification in this thesis will be done with the use of state space design and transfer functions. Chapter 4 explains state space design and the application to the first order linear model of the respiratory, thorax and lung mechanics. Chapter 5 discusses the results of system identification of the first order linear model. Chapter 6 describes the application of transfer functions for system identification of the first order linear model which is also described with the state space design. This chapter also elaborates on additional characteristics which can be explored using the transfer function. Lastly, the second order linear model is described and discussed. With chapter 7 the second part of the thesis begins. This chapter describes simulation of respiratory, thoracic and lung mechanics. These models are especially useful for the educational purposes described before. This chapter shows models with different levels of complexity and simulation examples of each model. Chapter 8 discusses the most important implications for future research. It elaborates on further validation, application and development of modelling.

ACKNOWLEDGEMENTS

In the first place I would like to thank Bram Schoe for introducing me to the field of the ICU and mechanical ventilation in my very first year of my master, then welcoming me for a 10 week internship in my second master year and of course my graduate internship. His enthusiasm for my thesis and his confidence in me have driven me to keep improving myself. I would like to thank Peter Somhorst for pushing me to be more critical of my work and for his essential feedback for the integration between the medical and technical fields. The last person which had an essential contribution to my thesis project is Kim Batselier. He made the complex theory of system identification comprehensible for me. Without him, I would not have grown this much in my technical skills.

A special thanks to Petra Rietveld and Willem Snoep for including me, teaching me bedside tricks and being my overall buddies during this year. I would like to thank the team of the ICU of the LUMC for accepting me and my new profession in the medical field. Lastly, I would like to thank my friends and family for their continuous support during my entire education but mostly in this last year. Without them, I would not have been able to start and finish this thesis.

Leiden, August 2020 Amne Mousa

NOTATION

ABBREVIATIONS

Abbreviation	Definition
$\mathbf{A}$	state matrix of state space design
ARDS	acute respiratory distress syndrome
$\mathbf{B}$	input matrix of state space design
BMI	body mass index
$\mathbf{C}$	output matrix of state space design
COPD	chronic obstructive pulmonary disease
COVID-19	coronavirus disease 2019
CT	computed tomography
$\mathbf{D}$	feed-through matrix of state space design
E	elastance
E_1	elastance of first compartment of two compartment model
E_2	elastance of second compartment of two compartment model
E_{CW}	chest wall elastance / thorax elastance
E_L	lung elastance
E_{RS}	respiratory system elastance
E_{Th}	chest wall elastance / thorax elastance
F	Laplace transform of time domain function f
FRC	functional residual capacity
G	transfer function
I	inertia
I_{RS}	respiratory system inertia
ICU	intensive care unit
K	steady state gain
LIP	lower inflection point
LUMC	Leiden University Medical Centre
$\mathbf{M}$	model or real system
MIMO	multiple input multiple output
MSE	mean square error
$\mathbf{N}$	real system
N	number of samples
P_0	resting pressure
P_{alv}	alveolar pressure
P_{atm}	athmospheric pressure
P_{AW}	airway pressure
P_{CW}	transmural pressure of chest wall / thorax
P_{es}	oesphageal pressure
P_L	transpulmonary pressure
P_{pl}	pleural pressure
P_{plat}	plateau pressure
PEEP	positive end expiratory pressure
R	resistance
R_1	resistance of first compartment of two compartment model
R_2	resistance of second compartment of two compartment model
R_{common}	common resistance
R_{CW}	chest wall resistance / thorax resistance

R_L	lung resistance
R_{RS}	respiratory system resistance
RS	respiratory System
s	seconds
SE	standard error
SISO	single input single output
SNR	signal to noise ratio
t	time
TOP	threshold opening pressure
u	input
$\mathbf{u}$	input vector
U	Laplace transform of input
UIP	upper inflection point
V	volume
$\ddot{V}$	acceleration of flow
$\dot{V}$	flow
$\dot{V}_1$	flow of first compartment of two compartment model
$\dot{V}_2$	flow of second compartment of two compartment model
V_{0_1}	resting volume of first compartment of two compartment model
V_{0_2}	resting volume of second compartment of two compartment model
V_{0_Th}	resting volume of thorax
V_0	resting volume
V_1	volume of first compartment of two compartment model
V_2	volume of second compartment of two compartment model
V_N	cost function
VILI	ventilation induced lung injury
$\mathbf{x}$	state vector
$\dot{\mathbf{x}}$	derivative of the state vector $\mathbf{x}$
y	output
$\hat{y}$	estimated output
$\mathbf{y}$	output vector
Y	Laplace transform of output
y_{ss}	steady state value
$\boldsymbol{\theta}$	parameter vector of real system
ϵ	error function
$\hat{\boldsymbol{\theta}}$	estimated parameter vector of model
σ	standard deviation
τ	time constant

CONVENTIONS

For equations, a bold uppercase letter represents a matrix and bold lowercase is a vector.

The unit for pressure is cm H_2O which is commonly used in mechanical ventilation (1 cm H_2O = 0.098 kPa). The pressures are referenced to atmospheric pressure, P_{atm} = 0 cm H_2O. Volume is expressed in litres (L). Flow is expressed in litres per second, (L s^{-1}). Positive values of flow indicate inspiratory flow and negative values of flow indicate expiratory flow. The elastance is a pressure per unit volume: cm H_2O L^{-1}. The resistance is given in cm H_2O s L^{-1}. Inertia is expressed as cm H_2O s^2 L^{-1}.

CONTENTS

Preface v
Notation vii

I INTRODUCTION

1 BACKGROUND 3
1.1 Mechanical ventilation . . . 3
1.2 Mathematical modelling . . . 4
2 THE RESPIRATORY MECHANICS 5
2.1 Balloon-pipe model . . . 5
2.2 Double balloon-pipe model . . . 6
2.3 Two compartment model . . . 7
2.4 Nonlinear lung mechanics . . . 8

II SYSTEM IDENTIFICATION

3 BACKGROUND 13
3.1 System identification and parameter estimation . . . 13
3.2 Parameter accuracy . . . 14
4 STATE SPACE DESIGN 15
4.1 Modelling respiratory mechanics . . . 15
4.1.1 Modelling from step experiment . . . 16
4.2 Modelling thoracic and lung mechanics . . . 18
4.3 Parameter accuracy . . . 18
5 PARAMETER ESTIMATION RESULTS 19
5.1 Data acquisition . . . 19
5.2 Respiratory system . . . 19
5.3 Thorax and lung . . . 22
6 TRANSFER FUNCTION 27
6.1 Modelling respiratory mechanics . . . 27
6.1.1 Modelling from step experiment . . . 27
6.2 Frequency response . . . 28
6.3 Second order linear model . . . 31
6.3.1 Estimation results . . . 31

III SIMULATION

7 MODEL DESIGN 37
7.1 Model 1: model of respiratory system . . . 37
7.2 Model 2: model of thorax and lung . . . 38
7.3 Model 3: model of heterogeneous lung . . . 39
7.4 Model 4: heterogeneous lung with recruitment . . . 40

IV FUTURE IMPLICATIONS

8 FUTURE IMPLICATIONS 45
8.1 Future research . . . 45
8.2 Further model development . . . 45

V APPENDICES

Part I

INTRODUCTION

1 BACKGROUND

1.1 MECHANICAL VENTILATION

Nearly 500 years ago, Andreas Vesalius was the first to suggest positive pressure as a method for ventilation of the lung for resuscitation [1]. It was not until the 20th century that mechanical ventilation was seen as a widely useful technique. The amount of patients in need for respiratory support during the polio epidemic in the 1950s lead to the first intensive care units (ICU) and mechanical ventilators as used today [2]. Over the past 70 years, safety and technology behind mechanical ventilators and insights of mechanical ventilation have increased majorly. Today, mechanical ventilation is one of the most frequently used techniques in intensive care medicine. It is a life-sustaining treatment for respiratory failure by reducing the work of breathing and providing gas exchange [2].

Ventilation is the process of moving air into and out of the lung to facilitate gas exchange of oxygen and carbon-dioxide. In healthy subjects, this process is primarily established through contraction of the diaphragm. The lung is attached to the thoracic cage and diaphragm by membranes: the pleurae. During an inhalation, the diaphragm contracts causing a negative intrapleural pressure. This negative intrapleural pressure causes a decrease in the intrapulmonary pressure or alveolar pressure. Difference between alveolar pressure and airway pressure causes air to flow in to the lung, until alveolar pressure and airway pressure are equal again. At the end of an inspiration the diaphragm relaxes, increasing alveolar pressure which causes air to flow out of the lung. This a form of negative pressure ventilation: the flow of air is created due to negative pressure [3]. The mechanical ventilators of today use positive pressure ventilation; they generate a pressure which increases the airway pressure resulting in a pressure difference between airway and lung. A mechanical ventilator can either replace (controlled ventilation) or support the ventilation of the patient. In this report, only controlled ventilation without any spontaneous muscle activity of the patient will be discussed. In the Netherlands, the most common used form of controlled ventilation is pressure controlled ventilation, where the observer determines the maximum pressure allowed [4].

A mechanical ventilator can produce higher volumes and pressures across the respiratory system than usually occur in healthy physiological breathing. The forces acting on (affected) lung tissue can be much greater due to inhomogeneous ventilation, i.e. the applied pressure and volume are not equally distributed across the respiratory system [5]. This can result in very high local pressures inducing lung injury. This ventilation induced lung injury (VILI) is one of the most important subjects in mechanical ventilation [2]. In 2000, The Acute Respiratory Distress Syndrome Network published a trial that showed the importance of lung protective ventilation [6]; by limiting the volumes delivered to the lung, the mortality rate decreased. It is therefore important to not only achieve adequate gas exchange but also to limit the VILI by limiting the amount of pressure and volume applied to the lung tissue.

1.2 MATHEMATICAL MODELLING

Breathing and mechanical ventilation are mechanical processes. The pressure, flow and volume during a breathing cycle are dependent on the mechanical properties of the respiratory system of each individual. Respiratory mechanics play an important role in occurrence of VILI. Through understanding of these respiratory mechanics, the effects of mechanical ventilation on lung tissue can be better understood [7]. Because mathematical models have potential to increase understanding of systems, the use of models of respiratory mechanics are thought to improve mechanical ventilation.

A model in the widest sense is a simplified representation of reality. The models in this thesis refer to mathematical models that are used in engineering and science to study physical systems. A system is an object where external stimuli - input signals - interact and produce observable signals - output signals [8]. Mathematical models describe the relation between input and output signals using mathematics. Complexity of a model is determined by the purpose of the model. For each research equation, it should be determined if the model is accurate enough to answer the research question.

There are roughly two ways of designing a model: system identification and simulation [8]. System identification will be used to determine accuracy of model structures and explore additional properties of the system. Simulation allows for easy visualisation of the effects of respiratory mechanics on mechanical ventilation. Simulation also allows to include theoretical concepts of respiratory mechanics described in literature, which can not be identified with the use of system identification. In the following chapters both methods are used for the modelling of respiratory mechanics.

2 THE RESPIRATORY MECHANICS

The respiratory system is not as such a black box but rather a grey box; there is some knowledge about the respiratory mechanics and thus about the structure of the model. The most important aspects of respiratory mechanics will be discussed.

2.1 BALLOON-PIPE MODEL

The respiratory mechanics describe the motion and deformation of tissue in relation to the flow of air. The relation between pressure, volume and flow can be described with the second order differential equation [7, 9]:

$$P_{AW}(t) = P_0 + E_{RS} \cdot (V(t) - V_0) + R_{RS}\dot{V}(t) + I_{RS}\ddot{V}(t) \tag{2.1}$$

P_{AW} is the airway pressure and P_0 is the pressure of the system at end expiration, which is considered to be the resting state of the system. The component of the respiratory system that is resistive to the acceleration of the flow, inertia, is depicted with parameter I_{RS}. Inertia is ought to be a parameter only of importance in high frequencies. Physiological respiratory frequencies are very low. Inertia is therefore seen as negligible, which is why the respiratory system is often depicted as a first order linear system [9]:

$$P_{AW}(t) = P_0 + E_{RS} \cdot (V(t) - V_0) + R_{RS}\dot{V}(t) \tag{2.2}$$

This system can be visualized as a balloon-pipe model, figure 2.1 [7]. The balloon represents the functional part of the lung - i.e. the alveoli which provide gas exchange - and the pipe represents the airways which connect the lung to the outside world. In mechanical ventilation the single pipe is connected to the mechanical ventilator. The respiratory airways are considered to be flow resistive. With each breath, the flow of air has to overcome the resistive forces of the respiratory airways. The lung tissue is volume-elastic, which causes the lung to inflate due to increase of pressure. Elastance (E_{RS}) and resistance (R_{RS}) are properties of the respiratory system [10]. These properties differ between age, sex, build and can change due to different pathologies or positioning. Asthma or chronic obstructive pulmonary disease (COPD) for example cause airway obstruction resulting in an increase of resistance. These are so called obstructive diseases. COPD often includes lung emphysema which causes lung elastance to decrease. Restrictive pathologies such as pulmonary oedema, lung fibrosis and pneumonia cause an increase of lung elastance [11]. In mechanical ventilation P_0 is not equal to the atmospheric pressure but is positive to prevent end expiratory collapse of the lung. This pressure is called positive end expiratory pressure (PEEP).

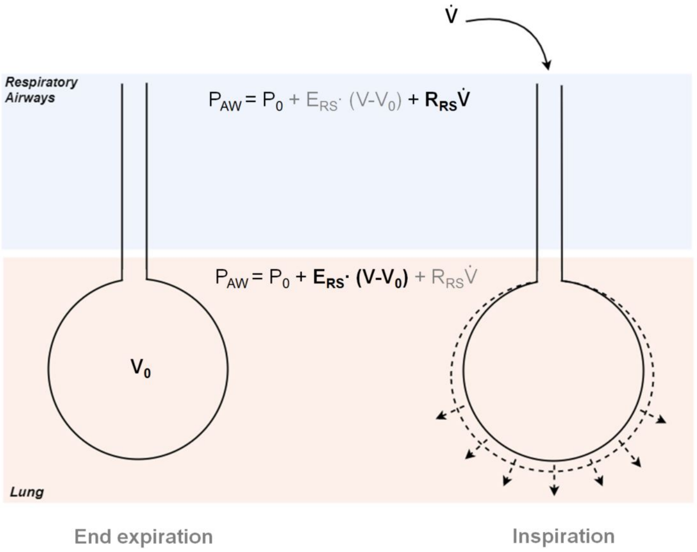
$\dot{V}$
Respiratory Airways
$P_{AW} = P_0 + E_{RS} \cdot (V-V_0) + R_{RS}\dot{V}$
$P_{AW} = P_0 + E_{RS} \cdot (V-V_0) + R_{RS}\dot{V}$
V_0
Lung
End expiration
Inspiration

Figure 2.1: The respiratory system as a balloon-pipe model. The pipe represents the respiratory airways which are flow resistive and the balloon represents the lung which is volume-elastic. End expiration is considered the resting state of the system with resting volume V_0 and resting pressure P_0. P_{AW} is the airway pressure. In mechanical ventilation, airway pressure is increased to generate a flow ($\dot{V}$). This increases alveolar pressure, thereby inflating the lung with a certain volume (V).

2.2 DOUBLE BALLOON-PIPE MODEL

In reality, the lung is connected to the thoracic cage with pleurae. Airway pressure is dependent on the combination and interaction between thorax and lung. Both lung and thorax have volume-elastic properties. The simple balloon-pipe model can be expanded with a thoracic cage: the double balloon-pipe model, figure 2.2.

From this model, lung elastance (E_L) and thorax elastance, also known as chest wall elastance (E_{CW}), can be individually determined, equation 2.3 and 2.4:

$$\begin{gathered} P_L(t) = P_0 + E_L \cdot \Big(V(t) - V_0\Big) \\ \text{with} \\ P_L = P_{alv} - P_{pl} \end{gathered} \tag{2.3}$$

and

$$\begin{gathered} P_{CW}(t) = P_0 + E_{CW} \cdot \Big(V(t) - V_{0\_Th}\Big) \\ \text{with} \\ P_{CW} = P_{pl} - P_{atm} \\ P_{CW} = P_{pl} - 0 \end{gathered} \tag{2.4}$$

where P_L is transpulmonary pressure: the transmural pressure of the lung. P_{CW} is the transmural pressure of the thorax. V_0 is the resting volume of the lung i.e. transpulmonary pressure is zero. For the thorax, V_{0_Th} is the volume when pleural pressure is zero. The thoracic cage has an elastic recoil directed outwards while the lung has its elastic recoil directed inwards. When the forces of the two are in equilibrium, the transpulmonary pressure is zero. The corresponding volume of this transpulmonary pressure is the function residual capacity (FRC) [3, 10].

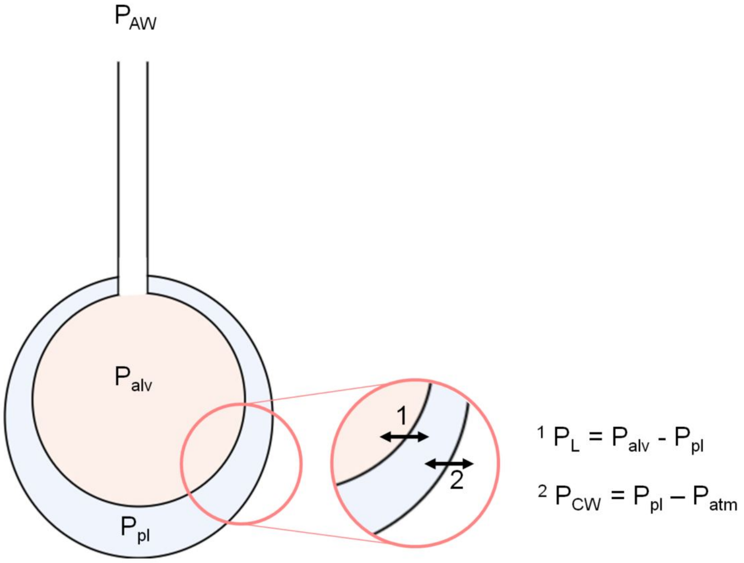

Figure 2.2: The pressures of the respiratory system. P_{AW} is the airway pressure. In positive pressure ventilation P_{AW} is increased to generate a pressure difference which allows ventilation. P_{alv} is the alveolar pressure or intrapulmonary pressure and P_{pl} the pleural pressure. The transmural pressures of the lung (P_L) and chest wall (P_{CW}) are the pressure differences across the tissues.

2.3 TWO COMPARTMENT MODEL

The models above assume that the lung has a single elastance and pleural pressures are similar across the thorax. This assumption is incorrect; there is a physiological pressure gradient of pleural pressures. The gravity pulls the lung downward, creating a greater vacuum at the top of the lung - the apex - resulting in a more negative pleural pressure. This results in different transpulmonary pressures across the lung with the same alveolar pressure [3]. Transpulmonary pressure differences can also occur in pathological lungs due to heterogeneity. The lung consists of many alveolar units, each with its own elastance. Total lung elastance is a summation of all individual alveolar units [7]. In a homogeneous lung, alveolar units are ought to have the same elastance. Many pathological lungs contain lung regions which are fully collapsed, full with fluid and lung regions which contain healthy lung tissue, see figure 2.3.

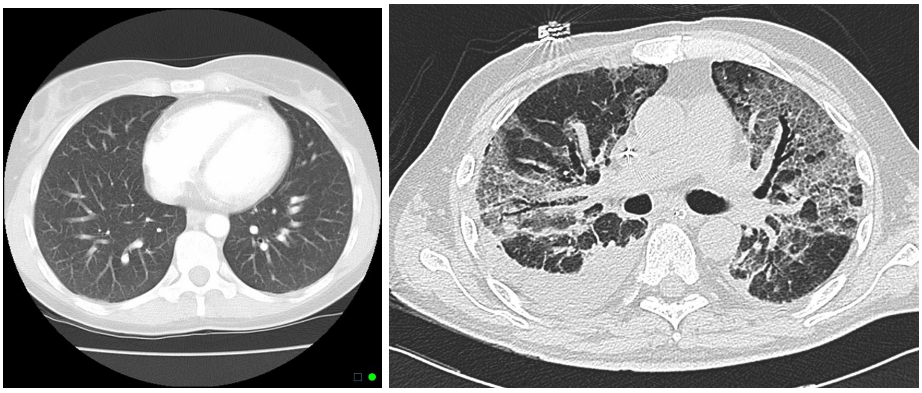

Figure 2.3: Computed Tomography (CT) of lungs: black indicates aerated tissue. Left: healthy lung tissue. Right: Affected lung tissue of ARDS with diffusely distributed deviations as well as pleural effusion. From Radiopaedia.org.

These differences in regional properties can be described with a two (or more) compartment model. The model describes a common resistance, from where the respiratory airways are divided in to two parts each with different resistance connected to lung tissue with different elastance. Local pressures can differ for each region; the effect of mechanical ventilation can therefore be different for each lung region. Total respiratory system elastance, resistance, volume and flow are a summation of the individual compartments:

$$\begin{gathered} P_{AW}(t) = \mathrm{PEEP} + (E_1 + E_2) \cdot \left(V_{total}(t) - V_0\right) + (R_1 + R_2)\dot{V}_{total}(t) \\ P_{AW}(t) = \mathrm{PEEP} + E_1 \cdot \left(V_1(t) - V_{0\_1}\right) + E_2 \cdot \left(V_2(t) - V_{0\_2}\right) + R_1\dot{V}_1(t) + R_2\dot{V}_2(t) \end{gathered} \tag{2.5}$$

2.4 NONLINEAR LUNG MECHANICS

Both elastance and resistance of the respiratory system do not behave as linear systems. The summation of the two results in the pressure-volume relationship of the respiratory system, figure 2.4.

The pressure-volume relationship of the lung is shown in figure 2.5. At high pressures, the slope of the graph decreases indicating increase of elastance caused by overdistension of the lung tissue [3]. In restrictive diseases the elastance is increased resulting in less volume with the same transpulmonary pressure. Diseases such as emphysema decrease elastance resulting in more volume with the same transpulmonary pressure.

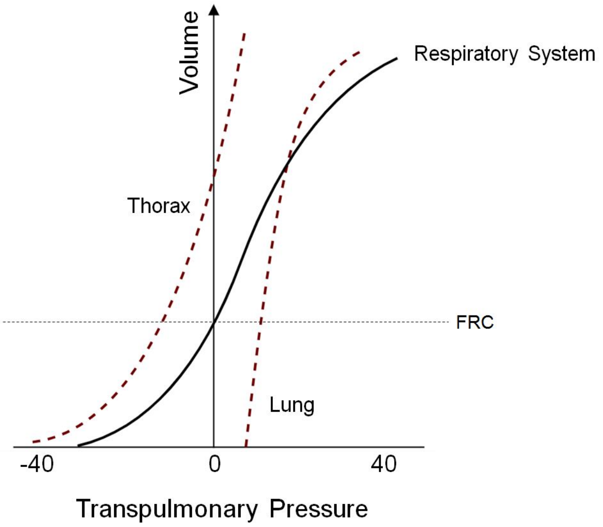

Figure 2.4: Pressure-volume relationship of thorax and lung. The summation of thorax and lung (red dashes lines) result in the pressure-volume relationship of the respiratory system (black line). The transpulmonary pressure is zero where the inward force of the lung is equal to the outward force of the thorax. The volume corresponding with a transpulmonary pressure of zero is the functional residual capacity (FRC) of the lung.

Figure 2.5 portrays the lung as a purely elastic material. In reality, both lung and thorax are not purely elastic materials but rather visco-elastic. Due to these properties the inspiratory and expiratory leg of the breathing cycle do not have the same pressure-volume relationship [12].

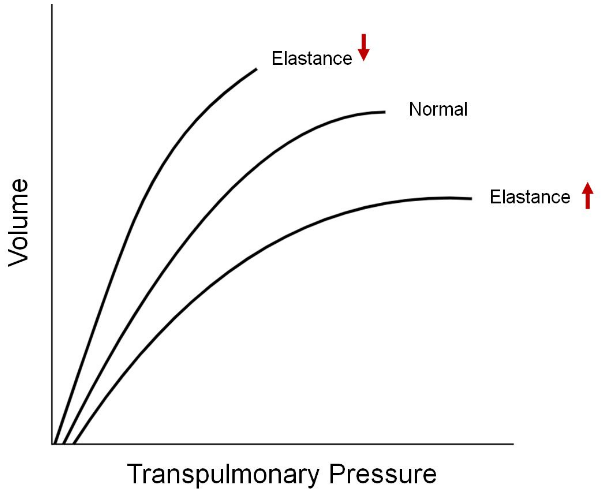

Figure 2.5: Pressure-volume relationship of healthy and affected lung. For both healthy and affected lung elastance increases at high pressures due to overdistension of the lung tissue. In restrictive diseases such as fibrosis the elastance increases resulting in less volume with the same transpulmonary pressure. Diseases such as emphysema decrease elastance resulting in more volume with the same transpulmonary pressure.

Due to this hysteresis, the actual volume at a given pressure depends on the direction from which that pressure is reached. The inspiratory leg shows high elastance at low transpulmonary pressures. This is assumed to be the result of collapsed alveoli, which have a high elastance. By increasing transpulmonary pressure, these collapsed alveoli are opened, i.e. recruited, resulting in an overall decrease of elastance. The point at which the elastance changes from high to low is called the lower inflection point (LIP). At the upper inflection point (UIP) the opened alveoli are assumed to be overdistended, resulting in a higher elastance. The expiratory leg shows lower elastance at same transpulmonary pressures due to the recruited alveoli during inspiration. In reality, recruitment and overdistension are not limited to the inflection points but occur during a breath.

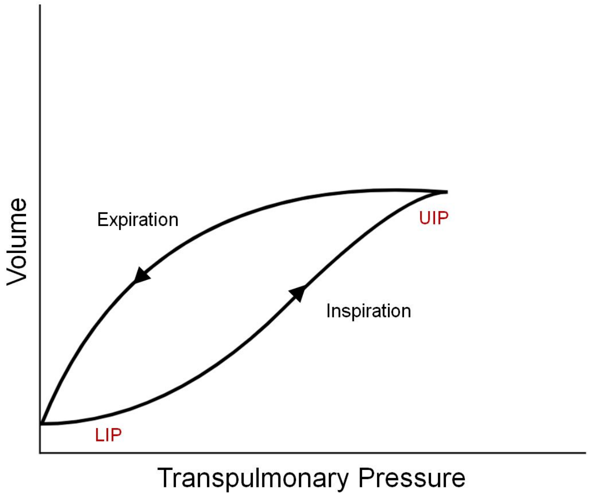

Figure 2.6: Pressure-volume relationship of the lung during inspiration and expiration. The inspiratory leg shows a lower inflection point (LIP), where elastance decreases due to recruitment of collapsed alveoli. At high transpulmonary pressures, the alveoli are overdistended resulting in higher elastance identified with the upper inflection point (UIP). The expiratory leg shows lower elastance at same transpulmonary pressures due to the recruited alveoli during inspiration.

Part II

SYSTEM IDENTIFICATION

3 BACKGROUND

3.1 SYSTEM IDENTIFICATION AND PARAMETER ESTIMATION

System identification is the process in which dynamic models are built based on measured input and output data. Figure 3.1 shows a schematic block diagram of system identification. The real physical system is described as system **N** with input u(t) and output y(t). The relation between input and output is determined by the structure and parameters of the system, represented with the parameter vector $\boldsymbol{\theta}$, equation 3.1. The mathematical model of system **N** is model **M** with simulated output $\hat{y}(t)$. The calculation of $\hat{y}(t)$ depends on the estimated parameter vector $\hat{\boldsymbol{\theta}}$ of **M**, equation 3.2:

$$y(t) = \mathbf{N}\left(\boldsymbol{\theta}, u(t)\right) \tag{3.1}$$

$$\hat{y}(t) = \mathbf{M}\left(\hat{\boldsymbol{\theta}}, u(t)\right) \tag{3.2}$$

In pressure controlled mechanical ventilation, the respiratory system is the real physical system **N** with pressure as input signal and volume as output signal.

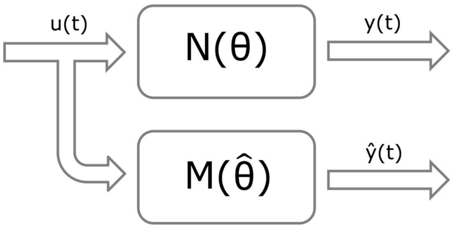

Figure 3.1: Block diagram of system identification. The real system is **N** with pressure as input u(t) and volume as output y(t). The relation between input and output is determined by the structure of the system and the parameters of the system, represented with the parameter vector $\boldsymbol{\theta}$. The estimated parameter vector $\hat{\theta}$ and the structure of **M** determine the simulated output $\hat{y}(t)$.

The relation between pressure and volume at each point in time is dependent on the respiratory mechanics of the individual. The aim is to find a model that accurately simulates $\hat{y}(t)$ with the least amount of parameters [13]. The difference between estimated and measured output is described with the error function, equation 3.3:

$$\epsilon(\theta) = y(t) - \hat{y}(\theta, t) \tag{3.3}$$

The performance of the model is evaluated with the use of the cost function which is the time average of the mean-square error (MSE) of the error function:

$$V_N\left(\mathbf{M}, \boldsymbol{\theta}, u(t)\right) = \frac{1}{N}\sum_{t=1}^{N}\left(y(t) - \hat{y}(\theta, t)\right)^2 \tag{3.4}$$

The objective of system identification is to minimise V_N by finding the optimal $\hat{\boldsymbol{\theta}}$, given the model structure and measured data:

$$\hat{\boldsymbol{\theta}} = \arg\min V_N\left(\boldsymbol{\theta}, u(t)\right) \tag{3.5}$$

The system identification problem can be solved manually or with the use of iterative search algorithms. Iterative search algorithms are algorithms that for each iteration change $\hat{\boldsymbol{\theta}}$ until the system identification problem, equation 3.5, is solved or rather minimised. If $\hat{\boldsymbol{\theta}}$ contains two parameters then a two dimensional plane describing each possible combination of parameter values is searched by the algorithm. [8].

3.2 PARAMETER ACCURACY

After finding parameter vector $\hat{\boldsymbol{\theta}}$ that minimizes V_N, it should be evaluated if the model is valid. The data sets are split is to two sets. The first set is used to determine the parameters (training data). The second data set is used to validate the model (validation data). With the identified parameters from the training data set, the output can be predicted using the input signal from the validation data set. The validation data set will be used to solve the cost function V_N, equation 3.4 to determine the accuracy of the model. To determine if the parameters are accurate, the standard error is calculated with the standard deviation:

$$\mathrm{SE} = \frac{1}{\sqrt{N}}\sigma \tag{3.6}$$

Even though the respiratory system is nonlinear, a linear model might be accurate enough to understand global mechanisms and simulate mechanical ventilation. Throughout the modelling of ICU patients it must be remembered that the estimated parameters from the system identification procedures are true for that moment in time. Due to development of the affected lung, hemodynamic changes, fluid balance, drug interactions or even the positioning of the patient in bed, the respiratory mechanics continuously change over time.

4 STATE SPACE DESIGN

4.1 MODELLING RESPIRATORY MECHANICS

The respiratory system as a first order linear system as shown in equation 2.2 with parameters E and R can be represented with a state space model. State space models express nt-order differential equations as systems with coupled first-order differential equations in matrix form. Figure 4.1 shows the block diagram corresponding to the state space model. The general form of state space models with p inputs and q outputs is shown in equation 4.1:

$$\begin{aligned} \dot{\mathbf{x}}\mathbf{(t)} &= \mathbf{Ax(t)} + \mathbf{Bu(t)} \\ \mathbf{y(t)} &= \mathbf{Cx(t)} + \mathbf{Du(t)} \end{aligned} \tag{4.1}$$

Here **x(t)** is the state vector containing n elements for a nth order system which describes the state of the system. The input matrix **A** is a $n \times n$ system matrix. The input matrix **B** is a $n \times p$ matrix and output matrix **C** is a $q \times n$ matrix. The direct feed-trough matrix **D** is a $q \times p$ matrix. The input vector **u(t)** contains all the input signals and **y(t)** contains the output signals. State space models are especially convenient for describing multiple-input multiple-output (MIMO) systems [14].

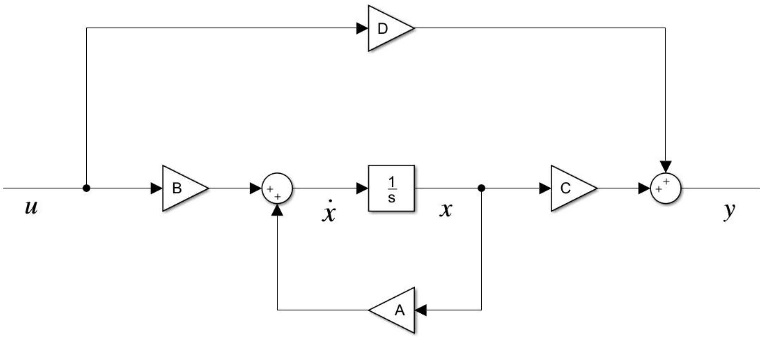

Figure 4.1: Block diagram of the state space model. The state matrices **A**, **B**, **C** and **D** contain the variables of the system. The input vector **u** contains all input signals and the output vector **y** contains all output signals.

The model of the respiratory system is a single-input single-output (SISO) system, where input is pressure applied by the mechanical ventilator and output is volume measured by the mechanical ventilator. By rewriting the first order differential equation as shown in equation 4.2, the state space representation of the balloon-pipe model can be deduced as can be seen in equation 4.3:

$$\begin{aligned} P_{AW}(t) &= P_0 + E \cdot (V(t) \text{ - } V_0) + R\dot{V}(t) \\ R\dot{V}(t) &= P_{AW}(t) - P_0 - E \cdot (V(t) \text{ - } V_0) \\ \dot{V}(t) &= -\frac{E}{R} \cdot (V(t) \text{ - } V_0) + \frac{1}{R} \cdot \left(P_{AW}(t) - P_0\right) \end{aligned} \tag{4.2}$$

$$\begin{aligned} \dot{\mathbf{x}}(t) &= \mathbf{A}x(t) + \mathbf{B}u(t) \\ \overbrace{\dot{V}(t)}^{\dot{x}(t)} &= -\underbrace{\frac{E}{R}}_{\mathbf{A}} \cdot \overbrace{(V(t) \text{ - } V_o)}^{x(t)} + \underbrace{\frac{1}{R}}_{\mathbf{B}} \cdot \overbrace{\left(P_{AW}(t) - P_o\right)}^{u(t)} \\ y(t) &= \mathbf{C}x(t) + \mathbf{D}u(t) \\ y(t) &= \overbrace{(V(t) \text{ - } V_o)}^{x(t)} \end{aligned} \tag{4.3}$$

For the first order linear model of the respiratory system, the input is P_{AW}-P_o and the output is V-V_o. The parameter matrices **A** and **B** are scalars in SISO systems. Parameter R can be directly extracted with the estimation of B:

$$\begin{aligned} B &= \frac{1}{R} \\ R &= \frac{1}{B} \end{aligned} \tag{4.4}$$

With the estimation of A and R, E can be deduced:

$$\begin{aligned} A &= \frac{-E}{R} \\ E &= -A \cdot R \end{aligned} \tag{4.5}$$

The output of the system, y(t), is equal to volume difference, x(t), making the **C** matrix equal to 1. The input has no direct influence on the output but rather through the state equation, making the **D** matrix equal to zero.

4.1.1 Modelling from step experiment

In pressure controlled ventilation, the pressure wave forms are similar to multiple unit step functions. A unit step function is a function where the values are 0 for $t < 0$ and 1 for $t > 0$, as can be seen in figure 4.2. The volume is thus a step response function, figure 4.3.

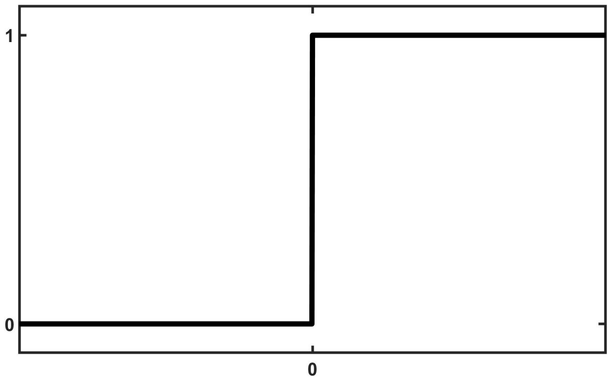

Figure 4.2: A unit step function. For $t < 0$, y is 0 whereas for $t > 0$ y is equal to 1.

For a linear state space model the step response is described by equation 4.6 [15]:

$$y(t) = \underbrace{\mathbf{CA}^{-1}e^{\mathbf{A}t}\mathbf{B}}_{\text{transient}} + \underbrace{\mathbf{D} - \mathbf{CA}^{-1}\mathbf{B}}_{\text{steady state}} \tag{4.6}$$

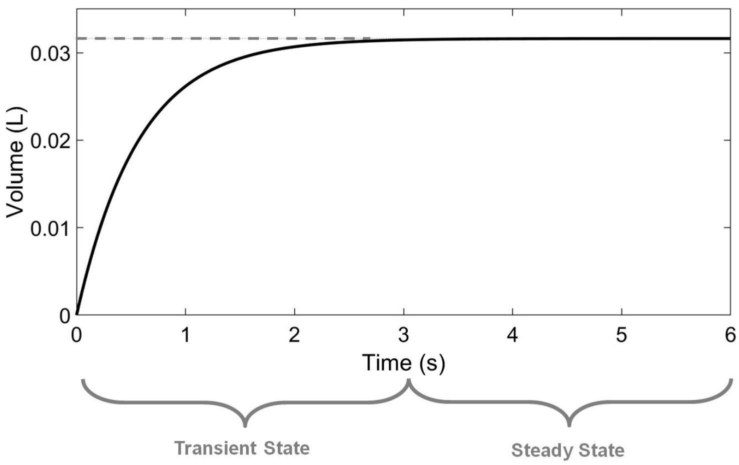

Figure 4.3: Example of step response function with a transient state and a steady state.

The first term, $\mathbf{CA}^{-1}e^{\mathbf{A}t}\mathbf{B}$, represents the transient response and determines how fast the steady state is reached. In a stable system this term decays to zero as t reaches the steady state. The second term, $\mathbf{D} - \mathbf{CA}^{-1}\mathbf{B}$, determines the amplitude of the steady state response.

For the linear model described in equation 4.3 the step response is dependent on the parameters as follow:

$$y(t) = \frac{-1}{E}e^{\frac{-E}{R}t} + \frac{1}{E} \tag{4.7}$$

The steady state value can be manually extracted from experimental data. From there E can be calculated:

$$y_{ss} = \frac{1}{E} \tag{4.8}$$

With the calculated elastance value, the resistance can be calculated; a point in time is chosen when the steady state value is not yet reached ($t < t_{SteadyState}$). For example, $t_{60\%}$ is the time where y is at 60 % of the steady state value:

$$y(t_{60\%}) = \frac{-1}{E}e^{\frac{-E}{R}t_{60\%}} + \frac{1}{E} \tag{4.9}$$

For this point in time R can be solved. This automatically means that the value of R is dependent on the time point chosen by the observer. To increase accuracy of the estimation of R, equation 4.9 can be solved for multiple time points each with a different value for R. For each estimation of R the cost function can be drawn. The most accurate estimation of R is depicted with the smallest MSE of all cost functions.

Note that in this model, E is directly differentiated from the volume at the end of an inspiration. This suggests that at end inspiration the output - i.e. volume - is only dependent on elastance. When looking at equation 2.2, this is only true when the flow reaches zero end inspiration; the term $R\dot{V}$ decays to zero too. Only then is E directly related to the end inspiratory volume. In an ideal situation, the step input is long enough to let the system reach a steady state. In many individuals during mechanical ventilation, the flow does not decay to zero at the end of inspiration. The steady state value is not reached. Calculation of elastance assuming that the end inspiratory volume is the steady state value leads to a systematic error in the estimation of E and therefore the estimation of R. Elastance is systematically overestimated and thus is resistance underestimated. In addition, in this model, parameters E and R are estimated solely from the inspiratory cycle of one breath. However inspiration is active whereas expiration is passive, leading to different flow patterns and thus different resistances. Modelling from the step experiment estimates inspiratory resistance rather than a mean resistance for the entire respiratory cycle. In addition, modelling from the step experiment is both time consuming and can easily lead to systematic errors (biased estimation). For this reason, optimisation algorithms are used to estimate the parameters. Automatic estimation in this report is done with the use of the Identification Toolbox of MATLAB 2019b (Mathworks, Natick, Massachusetts, United States of America).

4.2 MODELLING THORACIC AND LUNG MECHANICS

To determine individual properties of the thorax and lung described by equation 2.3 and 2.4, pleural pressures should be measured to determine thoracic properties and transpulmonary pressures for lung properties. The oesophageal pressure, P_{es}, is used in mechanical ventilation as a representation of pleural pressure [16, 17]. If $P_{pl} \approx P_{es}$, the model of the thorax can be deduced with the use of equation 2.4 and the model of equation 4.3:

$$\begin{aligned} \dot{x}(t) &= -\frac{E_{CW}}{R_{CW}} x(t) + \frac{1}{R_{CW}} \underbrace{u(t)}_{P_{es}} \\ y(t) &= x(t) \end{aligned} \tag{4.10}$$

With the oesophageal pressure curves the representation of the transpulmonary pressure can be calculated: $P_L \approx P_{AW}$ - P_{es}. For the lung model, this calculated transpulmonary pressure is used as input:

$$\begin{aligned} \dot{x}(t) &= -\frac{E_{L}}{R_{L}} x(t) + \frac{1}{R_{L}} \underbrace{u(t)}_{P_{AW}\text{ - }P_{es}} \\ y(t) &= x(t) \end{aligned} \tag{4.11}$$

Parameters E_{CW} and E_L are considered to be the elastance of the thorax and lung. Parameters R_{CW} and R_L are not considered to be purely flow resistive components as is the case in the respiratory system where respiratory airways are purely flow resistive. R_{CW} and R_L are resistive components due to viscous properties, whereas elastance represents elastic properties. Combining the two results in the the visco-elastic properties of the thorax and lung as discussed in chapter 2.

4.3 PARAMETER ACCURACY

To detect systematic errors the estimated elastance can be compared with the manually measured values of the elastance. In mechanically ventilated patients, the respiratory system elastance can be calculated:

$$E_{RS} = \frac{P_{plat}\text{ - PEEP}}{\Delta V} \tag{4.12}$$

P_{plat} is the plateau pressure, which is the airway pressure during an inspiratory occlusion manoeuvre. This causes the flow to decay to zero thereby eliminating pressure needed to overcome the resistive forces. Note that this is a static elastance measured at that moment in time. In the models described above estimated elastance will be an average elastance over time. It is expected that these two values have some differences. This is however a sufficient approach to evaluate if $\hat{\theta}$ is biased.

5 PARAMETER ESTIMATION RESULTS

5.1 DATA ACQUISITION

Data were extracted for five COVID-19 adult patients from the first of April until June 31^{st} at the ICU in the Leiden University Medical Centre (LUMC). All patients were sedated and received neuromusculair blockades. The patient characteristics relevant for respiratory mechanics are shown in table 5.1.

Table 5.1: Patient characteristics of five patients with COVID-19 pneumonia for system identification. BMI = body mass index, RS = respiratory system

Subject #	BMI	Prone positioning	Pulmonary history	Elastance RS
1	31.8	No	None	36
2	30.8	No	Asthma	35
3	26.8	No	Asthmatic bronchitis	20
4	19.4	No	None	45
5	31.4	Yes	None	30

Patient characteristics are included to determine if estimated parameters are in agreement with pathophysiological processes of the respiratory mechanics. Patient 2 and 3 have a history of asthma and asthmatic bronchitis. This can lead to a higher airway resistance. However, when treated properly the respiratory resistance can be normal as is the case in these subjects. No patients had a history of affected lung tissue. It is therefore expected that all patients have normal to increased lung elastance due to COVID-19 pneumonia. Body mass index (BMI) and prone positioning have a possible influence on elastance of the thorax. A high BMI can indicate obesity, which can result in increased thoracic elastance due to the amount of extra mass that should be inflated with each breath and/or increased abdominal pressure [18]. Prone positioning also leads to an increase of thoracic elastance [19].

For each patient, data files were extracted from the mechanical ventilator. All patients had an oesophageal balloon in situ, allowing for system identification of thorax and lung. Oesophageal balloons were positioned and calibrated by the investigator. All data files were analysed and cut by the investigator to exclude any artefacts for system identification procedures. The prepped pressure, flow and volume curves are shown in Appendix B. Elaboration of the MATLAB scripts for the preprocessing steps and system identification procedures can be found in Appendix C.

Static elastance of thorax and lung were not measured. Reference values for thorax and lung elastance are adapted from literature. In the study of van der Zee et al. [20] the mean lung elastance for COVID-19 pneumonia was 12 (9-23) cm H_2O L^{-1} and for thorax elastance 8 (5-19) cm H_2O L^{-1}.

5.2 RESPIRATORY SYSTEM

The results of system identification and parameter estimation of the respiratory system with automatic optimisation procedures are shown in table 5.2.

MSE and fit percentage are calculated with the use of validation data. The MSE values are small which means that the model can accurately simulate the volume

Table 5.2: Estimation results of system identification of the first order linear model of the respiratory system. MSE = mean square error. SE = standard error.

Respiratory System				
Subject #	MSE	Fit %	Elastance (SE)	Resistance (SE)
1	0.0029	64	32 (1.4)	18 (0.9)
2	7.4^{-04}	82	37 (0.7)	10 (0.3)
3	1.1^{-04}	93	23 (0.04)	10 (0.03)
4	0.0011	75	50 (0.9)	12 (0.5)
5	6.0^{-04}	83	35 (0.2)	12 (0.1)

response during mechanical ventilation. Patient 1 shows a MSE of 0.0029, meaning that the mean error is 29 millilitres which is a very small amount, however the fit in this patient is low. This is due to the fact that the human respiratory system is not an ideal system. In figure 5.1 measured and simulated volume of subject 1 is shown. The most probable reason of the bad fit can be seen in the end expiratory phase. This figure shows that for this subject, expiratory volume is smaller than inspiratory volume. Therefore, the expiratory limb does not return to zero. The model is an ideal system where inspiratory and expiratory volume are the same. This results in a difference between the model and the real system. Figure 5.2 shows the results of subject 4, which shows also a low fit due to the expiratory limb. In this case however, expiratory volume is larger than inspiratory volume. This leads to the expiratory limb to become negative leading to a difference between measured volume and simulated volume.

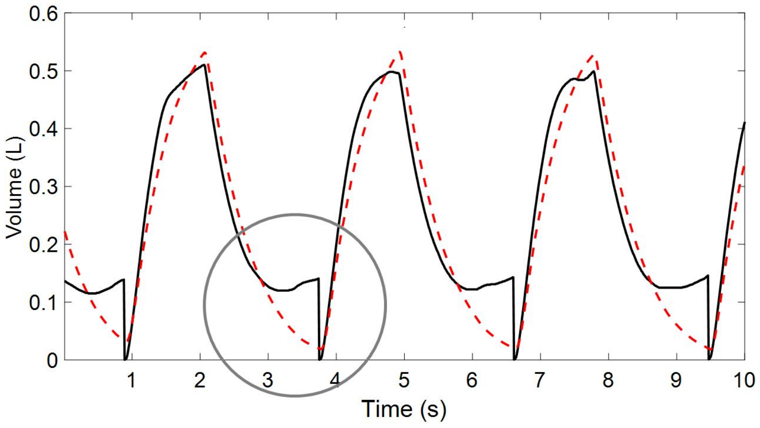

Figure 5.1: Measured volume (solid black line) and simulated volume (dashed red line). Expiratory volume of the measured data is smaller than inspiratory volume. This causes the expiratory limb to not return to zero leading to a decrease of overall fit.

Differences between inspiratory and expiratory volume can be due to multiple reasons. First, measured volume includes only volume which flows across the flow sensor which is located at the end of the endotracheal tube. In some cases, the flow of air leaks around the breathing circuits and thus does not cross the flow sensor, resulting in a smaller expiratory volume. Second, inspiratory air is usually at a different temperature than the temperature of the patient. Although the flow of air is warmed up before it reaches the patient, it loses heat due to the flow through breathing circuits. When the air reaches the patient, it is warmed up by body heat of the patient. According to the ideal gas law, an increase of temperature of gas leads to an increase of volume and/or pressure. This can result in a larger expiratory volume than inspiratory volume. Lastly, composition of air is also different due to gas exchange that occurs in the lung, leading to a volume difference. To increase the fit of the model, these phenomena should be taken in to account. However,

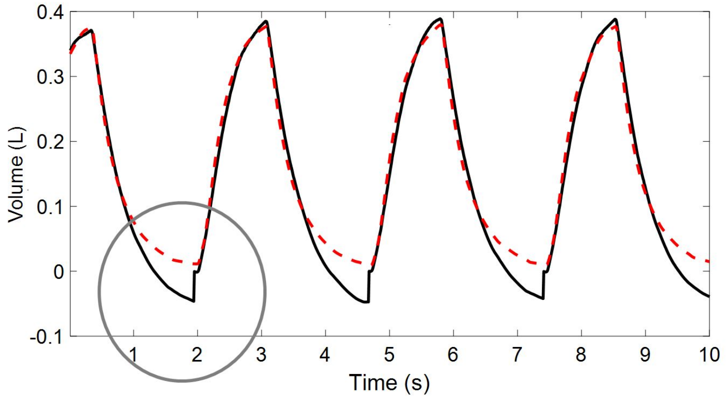

Figure 5.2: Measured volume (solid black line) and simulated volume (dashed red line). Expiratory volume of measured data is larger than inspiratory volume. This causes the expiratory limb to become negative whereas the simulated volume returns to zero. This causes overall fit to decrease.

these are very complex and nonlinear components. It is therefore more preferable to evaluate the bad fit percentages manually. If the shape (transient response) of inspiratory and expiratory leg of the volume curve have a good fit, the linear model approaches respiratory mechanics with high accuracy. Absolute volume differences can usually be explained by causes which are not related to respiratory mechanics. If the shape of simulated inspiratory or expiratory limb is different, the linear model is not sufficient. A possible reason for this can be that non-linearity of respiratory mechanics plays a more prominent role in the system.

The standard errors of estimated parameters are very small meaning that the estimation of the parameters are accurate. The agreement of the measured static elastance and estimated elastance is shown with a Bland-Altman plot, figure 5.3. The number of patients included is too small to determine if the agreement between the two measures is sufficient. It does allow for a clear visualisation of discrepancies. The mean of the difference between the two measures is -2 cm H_2O L^{-1}, meaning that estimated elastance is overall higher than measured elastance. Measured elastance was calculated with the use of expiratory volume. As described above, expiratory volume is usually larger than inspiratory volume. The model tends to fit to inspiratory volume since expiratory volume gets negative which is not possible in the ideal system of the model. Due to this difference, volume used in the measured elastance tends to be higher resulting in a lower elastance value. For patient 1, measured elastance is lower than estimated elastance. In this patient, expiratory volume is smaller resulting in a higher measured elastance. It is most likely that estimated elastance is more accurate for this patient since the calculated elastance does not take the air leak in to account.

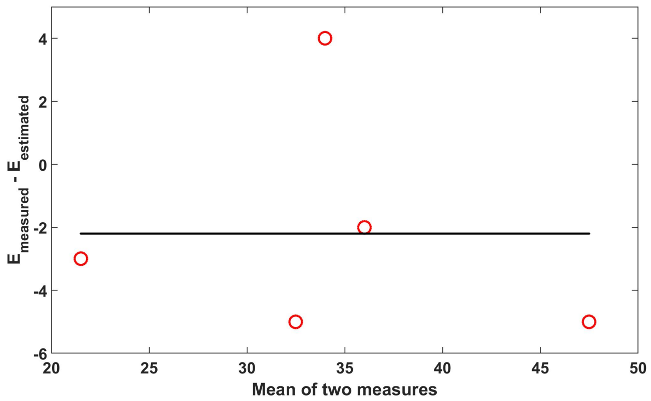

Figure 5.3: Bland-Altman plot of measured static elastance and dynamic estimated elastance of the respiratory system. The mean of the difference between the two measures is -2 cm H_2O L^{-1}, meaning that estimated elastance is overall higher than measured elastance.

5.3 THORAX AND LUNG

The results of system identification and parameter estimation of the thorax and lung with automatic optimisation procedures are shown in table 5.3 and 5.4.

Table 5.3: Estimation results of system identification of the first order linear model of the thorax. MSE = mean square error. SE = standard error.

Thorax				
Subject #	MSE	Fit %	Elastance (SE)	Resistance (SE)
1	0.0029	64	9 (0.2)	1 (0.1)
2	8.6^{-04}	80	11 (0.2)	1 (0.07)
3	0.0076	42	6 (0.10)	1 (0.06)
4	0.0087	30	10 (0.7)	1 (0.1)
5	0.01	29	5 (0.2)	1 (0.2)

Table 5.4: Estimation results of system identification of the first order linear model of the lung. MSE = mean square error. SE = standard error.

Lung				
Subject #	MSE	Fit %	Elastance (SE)	Resistance (SE)
1	0.0012	77	29 (0.6)	15 (0.5)
2	0.0011	77	26 (1.0)	10 (0.4)
3	2.3^{-04}	90	20 (0.07)	10 (0.04)
4	0.0011	75	50 (1)	12 (0.7)
5	9.1^{-04}	79	34 (0.3)	12 (0.1)

Estimated elastance values of the thorax do appear to be similar to the values of the study of van der Zee et al. [20]. Elastance values of the lung seem to be too high.

The assumption is made that both lung and thorax behave linear. The respiratory system is then a summation of the two systems. However in all subjects except for subject 2, summation of elastance values of thorax and lung does not result in the elastance value of the total respiratory system. The difference between the summation of thorax and lung and respiratory system is visualised with Blant-Altman plots, figure 5.4.

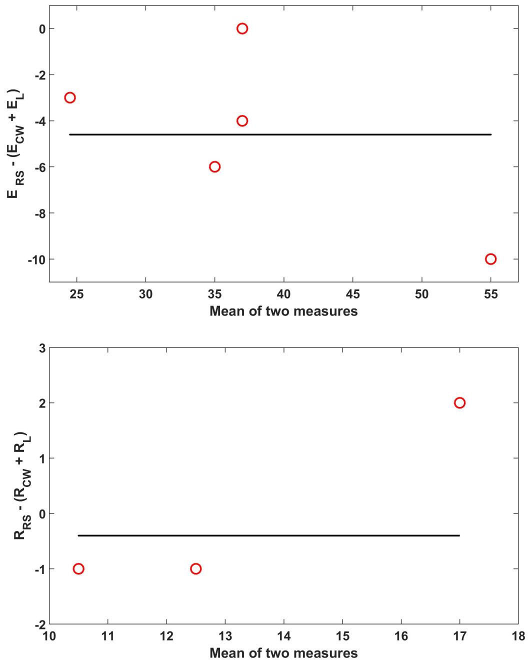

Figure 5.4: Bland-Altman plots of difference between estimated resistance and elastance of the respiratory system and the summation of estimated thorax and lung elastance and resistance. If the systems are estimated accurately and behave linear, the two values should agree.

As described before, it can be concluded that the estimation of the respiratory system is accurate which means that the error of summation lies within estimation using oesophageal pressures or the systems do not behave linear.

The discrepancies are most likely due to the noisy signals of the oesophageal pressures. Figure 5.5 shows oesophageal pressure curves of subject 4. Oesophageal pressure increase caused by alveolar pressure increase are indicated with red arrows. The other peaks identified with red dots are due to increase of pressure due to cardiac activity, also known as cardiac noise. In this case, cardiac noise is half the amplitude of the signal amplitude resulting in a low signal-to-noise ratio (SNR). Figure 5.6 shows input and estimated output signals of subject 2; the input signal has a better SNR leading to a better estimation of parameters and simulation of output.

To increase fit, oesophageal pressure curves can be filtered to increase SNR. With this, estimation results should improve. If not, there are additional reasons for a bad fit. It is possible that a linear model is not accurate enough to approach the non-linearity of the lung and/ or thorax. Therefore summation of elastance and resistance of thorax and lung do not add up to the estimated values of the respiratory system. It is also assumed that the oesophageal balloon gives an accurate approximation of pleural pressure across the lung. This can differ for each patient. In addition, positioning and calibration of the balloon can be difficult.

Even though oesophageal signals are also used to estimate lung parameters, the fit of the lung model is overall better than the model of the thorax. This is due to the fact that airway pressure curves have better signal-to-noise ratio than oesophageal pressure curves. Transpulmonary pressure is a resultant of the two signals thereby increasing SNR compared to oesophageal pressure curves. Even though SE of the parameters are small, estimated elastance values of the lung are almost equal to elastance values of the respiratory system for each subject. This would mean that all pressure applied to the respiratory system is applied to the lung and no pressure is applied to the thorax, which is not physiologically not possible. It can therefore

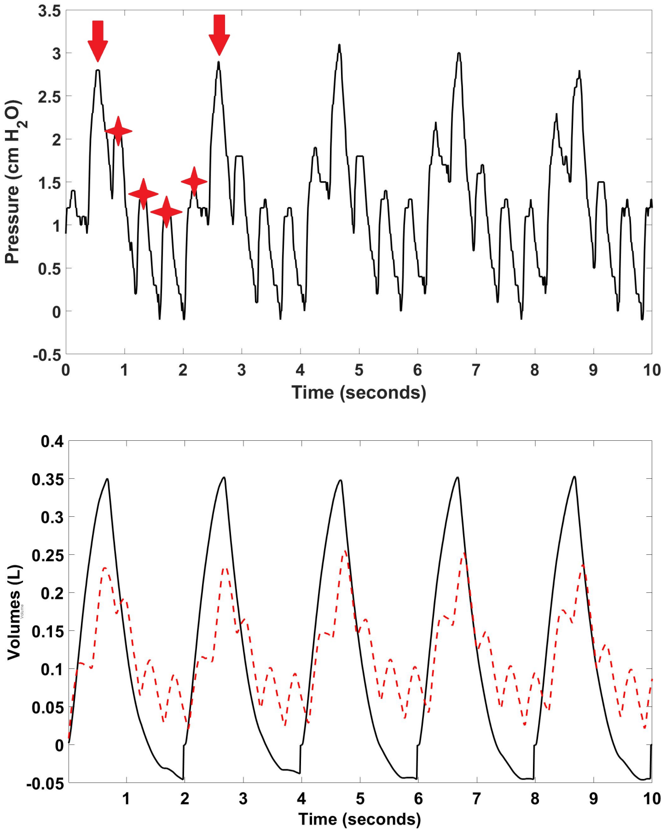

Figure 5.5: Upper figure: oesophageal pressure curves of subject 4. Pressure peaks indicated with arrows show increase of pressure due to increase of alveolar pressure during an inspiration. Pressure peaks indicated by red dots are due to cardiac activity also known as cardiac noise. The amplitude of cardiac noise is approximately half the amplitude of the pressure peaks of the inspiration resulting in a low signal-to-noise ratio. Lower figure: measured (black solid line) and estimated (red dashed line) volume. Noisy input signals lead to a bad estimation of parameters and bad simulation of output.

be concluded that the lung model is also not an accurate representation of lung mechanics.

Main findings:

- The first order linear model of respiratory mechanics is an accurate representation of the respiratory system of COVID-19 patients.
- Lung and thoracic mechanics can not be modelled with the first order linear model due to noisy input signals from the oesophageal pressure curves.

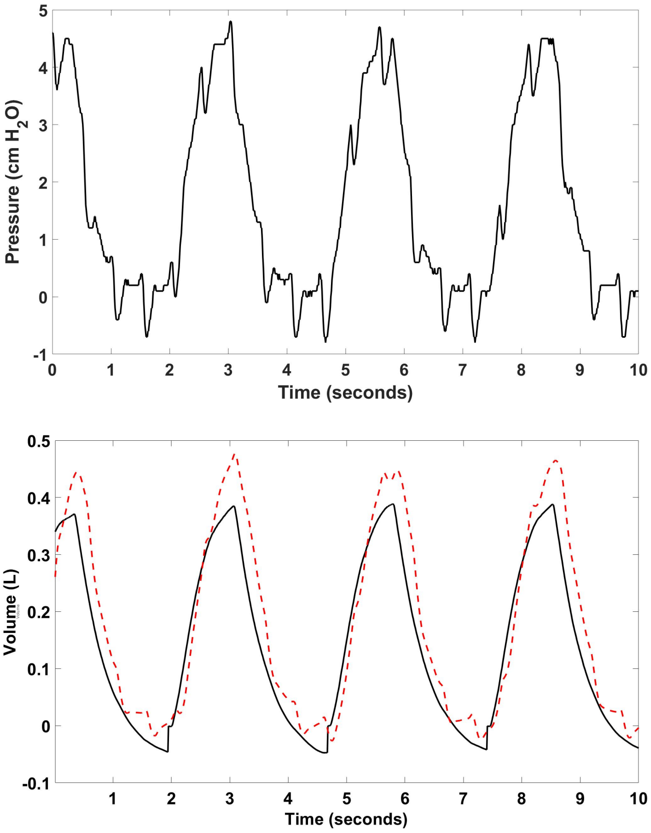

Figure 5.6: Upper figure: oesophageal pressure curves of subject 2. Lower figure: measured (black solid line) and estimated (red dashed line) volume. In comparison with subject 4, figure 5.5, signal-to-noise ratio is much better resulting in a better estimation of parameters and output.

6 TRANSFER FUNCTION

6.1 MODELLING RESPIRATORY MECHANICS

For linear models with one input and one output, the system can also be represented with a transfer function, figure 6.1. Transfer functions describe the relation between input and output in the Laplace domain, equation 6.1. Background theory of the Laplace transform can be found in Appendix A.

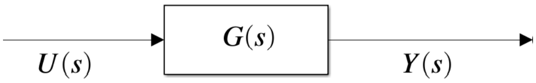

Figure 6.1: Block diagram of the transfer function. U(s) is the Laplace transform of input signal u(t) and Y(s) is the Laplace transform of output signal y(t). G(s) represents the transfer function of the system.

$$Y(s) = U(s)G(s) \tag{6.1}$$

Y(s) is the Laplace transform of y(t), U(s) the Laplace transform of u(t) and G(s) is the transfer function. For a first order linear differential equation the general form of the transfer function is:

$$G(s) = \frac{b_0}{s + a_0} \tag{6.2}$$

The transfer function of the balloon-pipe model with parameters E and R can be deduced to the general form of equation 6.2:

$$\begin{gathered} U(s) = E_{RS}Y(s) + R_{RS}sY(s) \\ U(s) = (E_{RS}{+}R_{RS}s)Y(s) \\ \frac{Y(s)}{U(s)} = \frac{1}{R_{RS}s + E_{RS}} \\ \frac{Y(s)}{U(s)} = \frac{1/R_{RS}}{s + (E_{RS}/R_{RS})} \end{gathered} \tag{6.3}$$

System identification estimates the values of b_0 and a_0 of equation 6.2. After parameter estimation the numerator (b_0) is directly related to parameter R and parameter E can be deduced from the denominator. The first order linear model of thorax and lung can also be expressed with transfer functions as follow:

$$\frac{Y(s)}{U(s)} = \frac{1/R_{CW}}{s + (E_{CW}/R_{CW})} \tag{6.4}$$

$$\frac{Y(s)}{U(s)} = \frac{1/R_L}{s + (E_L/R_L)} \tag{6.5}$$

6.1.1 Modelling from step experiment

Transfer functions of linear first order differential equations can also be determined with the step experiment as described before in section 4.1.1. To estimate parameters

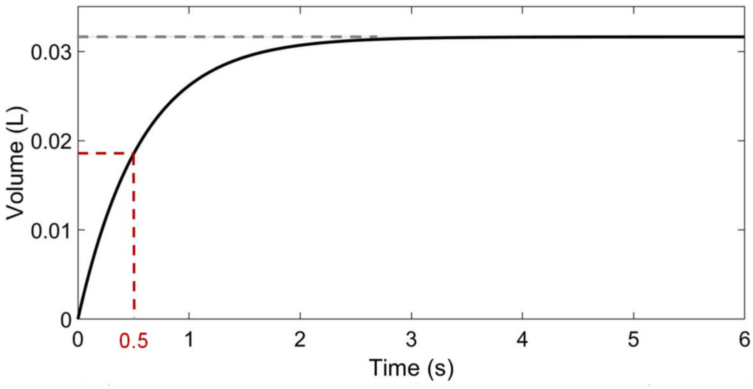

Figure 6.2: Step response of first order linear system. τ can be determined at 63% of the steady state, K. In this example, τ is 0.5 seconds.

from the step experiment it is convenient to use another general form for describing a first order linear model:

$$\begin{aligned} G(s) &= \frac{K}{\tau s + 1} \\ \text{where } a_0 &= \frac{1}{\tau} \text{ and } b_0 = \frac{K}{\tau} \end{aligned} \tag{6.6}$$

K is the steady state value of the step response and τ the time constant of the system. The transient state of the step experiment is dependent on τ. After τ seconds, the system is at 63% of the steady state value, as can be seen in figure 6.2. The steady state value is reached after five times the value of τ [15]. With use of equation 6.3 and 6.6, the relation between τ and K and parameters E and R can be determined, as can be seen in equation 6.7 and 6.8.

$$\begin{aligned} a_0 &= \frac{E}{R} = \frac{1}{\tau} \\ \tau &= \frac{R}{E} \end{aligned} \tag{6.7}$$

and

$$\begin{aligned} b_0 &= \frac{1}{R} = \frac{K}{\tau} \\ R &= \frac{\tau}{K} \\ K &= \frac{1}{R} \cdot \frac{R}{E} = \frac{1}{E} \end{aligned} \tag{6.8}$$

Equation 6.8 shows that the steady state value is directly dependent on elastance, which is also stated in the step experiment of the state space model. The estimated value of E will again lead to a systematic error, because the steady state value is usually not reached at the end of inspiration. The transient response is dependent on both elastance and resistance since τ is dependent on both parameters. In comparison with the step experiment from the state space model, the step experiment with the transfer function gives more insight of the influence of the parameters in the transient state. For example, an increase of resistance or a decrease of elastance results in a higher τ, which means that it takes longer to reach the steady state.

6.2 FREQUENCY RESPONSE

The results of chapter 5 suggest that the first order linear model is accurate for simulation of the respiratory system. With the transfer function, the model can be further explored to research characteristics about the respiratory system which could be relevant for mechanical ventilation. The transfer function allows for analysis of the system in the frequency domain. In controlled ventilation, the clinician determines respiratory frequency. Understanding the frequency response of the system can therefore be useful in decision making of ventilator settings.

When s is replaced by $j\omega$, $G(s) \rightarrow G(j\omega)$, the frequency response can be evaluated. Frequency response is often analysed with the use of a Bode plot. Additional background information of the Bode plot can be found in Appendix A. An example of a Bode plot of the first order linear model of the respiratory system is shown in figure 6.3. This figure shows that for all frequencies the magnitude is negative, meaning that input amplitude is reduced by the system. The higher the frequencies become, the more the input amplitude is reduced. The phase plot shows that the output lags the input, meaning there is some time delay in the response of the system.

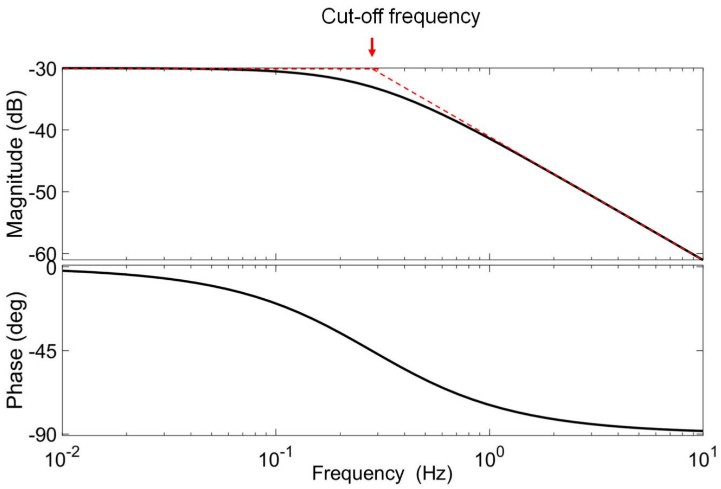

Figure 6.3: Example of Bode plot with magnitude in dB and phase in degrees. The magnitude for all frequencies is negative, meaning that amplitude of the input is reduced in the output. With higher frequencies, the magnitude becomes more negative. The phase plot shows a phase difference between input and output. A negative phase means that the output lags the input. Cut-off frequency is the frequency in which the magnitude is decreasing with a steady slope.

For mechanical ventilation frequencies of interest are respiratory frequencies. Input signals for Bode plots are sinusoidal waves, whilst input signals in mechanical ventilation are a pulse train. Every periodic signal can however be manufactured with a summation of sinusoidal waves with different frequencies. Figure 6.4 is the Fourier spectrum of the input in mechanical ventilation. A Fourier spectrum shows sinusoidal frequencies of which the signal is made out of. The fundamental frequency is the lowest frequency. In the pulse train for mechanical ventilation the fundamental frequency is the respiratory frequency and has the highest amplitude and thus has the most influence during mechanical ventilation. Figure 6.4 shows that all frequencies in input signals for mechanical ventilation are low. For pressure controlled ventilation the range of fundamental/respiratory frequencies lie within the range of 0.3 - 0.6 Hz.

Bode plots of all five COVID-19 patients are shown in figure 6.5. Figure 6.5 shows that cut-off frequencies lie within the range of physiological respiratory frequencies, meaning that volume decreases with higher frequencies in mechanical ventilation. Figure 6.6 shows Bode plots zoomed in for respiratory frequencies. The magnitude before cut-off frequencies is primarily dependent on elastance of the respiratory system. Patient 3 had a low elastance resulting in a less negative magnitude in comparison with the other patients, while patient 4 with a high elastance has a more negative magnitude. Cut-off frequency is dependent on τ; a higher time constant will lead to a lower cut-off frequency. At this frequency the phase difference also

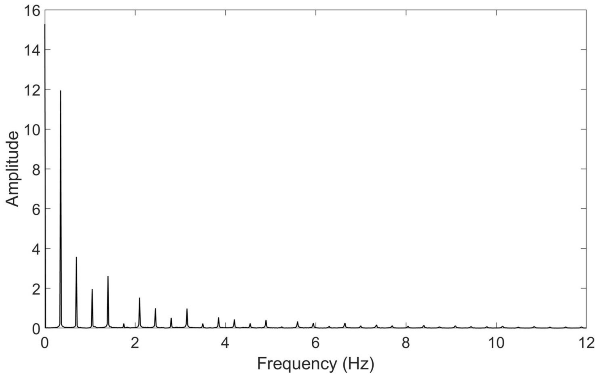

Figure 6.4: Example of Fourier spectrum of pressure waves used as input signal in mechanically ventilated patient in pressure controlled ventilation. X-axis is the frequencies. Y-axis is the amplitude of corresponding frequency. In this example, the patient was ventilated with a respiratory frequency of 21 breaths per minute or 0.35 Hz which has the highest amplitude. This means that the respiratory frequency.

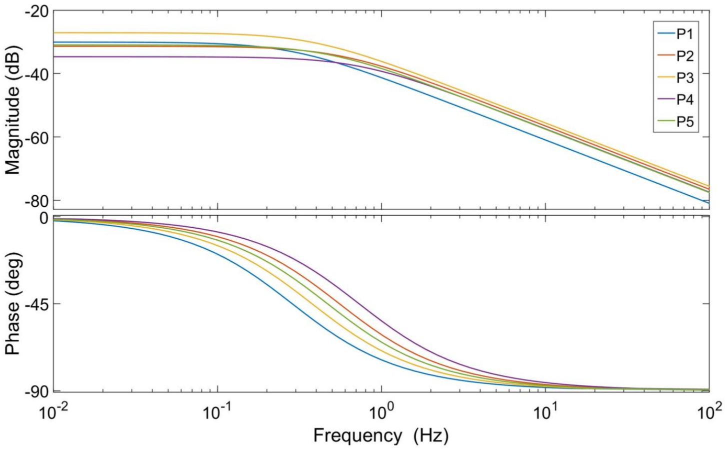

Figure 6.5: Bode plots of the five patients with COVID-19 pneumonia. Differences in Bode plot are explained by differences in respiratory mechanics. Before the cut-off frequency, magnitude is determined by elastance; a high elastance leads to a more negative magnitude. After the cut-off frequency the magnitude becomes more negative with a steady slope.

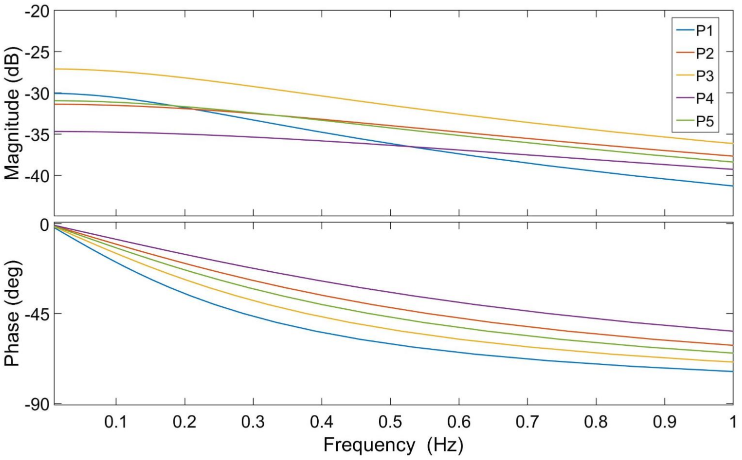

Figure 6.6: Bode plots zoomed in for the respiratory frequencies.

starts. This means that in respiratory frequencies higher than the cut-off frequency volume will decrease with a steady slope, as can be seen in figure 6.5. There will also be a delay between applied pressure and built up of volume. Time constants shown in table 6.1 are calculated with the use of estimated parameters from chapter 5. With a higher time constant, the system needs more time to reach steady state. If these subjects breath with higher respiratory frequencies, the system cannot reach steady state resulting in lower magnitude of output signal. Patients with spontaneous breathing activity will therefore prefer low respiratory frequencies to allow for full inflation of lung. Figure 6.6 shows that patient 1 with a high time constant is more sensitive for higher frequencies due to the low cut-off frequency. This is important to be aware of in the clinical setting. When there is a need for more alveolar ventilation, for example due to high levels of carbon-dioxide, respiratory frequency can be increased. However, an increase of respiratory frequency also leads to a decrease of tidal volume. There is a balance between optimum tidal volume and respiratory frequency. In controlled ventilation, a clinician should be alert of the time constant to determine if the subject is sensitive for high respiratory frequencies. For patients with a high time constant this optimum will lie with lower respiratory frequency. Increasing respiratory frequency in these patients will be counter productive and thus will result in less effective treatment.

Table 6.1: Time constant calculated with the estimated values of elastance and resistance according to equation 6.7 and table 5.2.

Subject #	Time constant (s)
1	0.56
2	0.27
3	0.43
4	0.24
5	0.34

6.3 SECOND ORDER LINEAR MODEL

Until now the respiratory system is approached as a first order linear system. Inertia is assumed to play a non significant role in low respiratory frequencies. This conclusion is based on experiments with healthy subjects [21]. Influence of inertia in patients can be explored with the second order linear model. The transfer function of this model is as follow:

$$\begin{aligned} \frac{Y(s)}{U(s)} &= \frac{1}{I_{RS}s^2 + R_{RS}s + E_{RS}} \\ \frac{Y(s)}{U(s)} &= \frac{1/I_{RS}}{s^2 + (R_{RS}/I_{RS})s + (E_{RS}/I_{RS})} \end{aligned} \tag{6.9}$$

Parameters can again be extracted from the identified system. Inertia of the respiratory system can be extracted from the numerator. Resistance can be deduced with the second term of the denominator and elastance with the third term of the denominator using the estimated value of inertia.

6.3.1 Estimation results

Estimation of the second order linear model introduces some extra difficulties. In the first order linear model, air leak result in an estimation error. By manually evaluating this error, the model is still concluded to be accurate. In the second order linear system this air leak prevents identification of the system, figure 6.7. Therefore, the data set is further preproccesed by interpolation of end expiratory phase. This prepocessing step is explained in Appendix D. Note that this interpolation decreases tidal volume; about 100 ml of volume will be cut away from the signal. This will lead to an overestimation of elastance since the same pressure will result in less volume. The system was identified with the interpolated data.

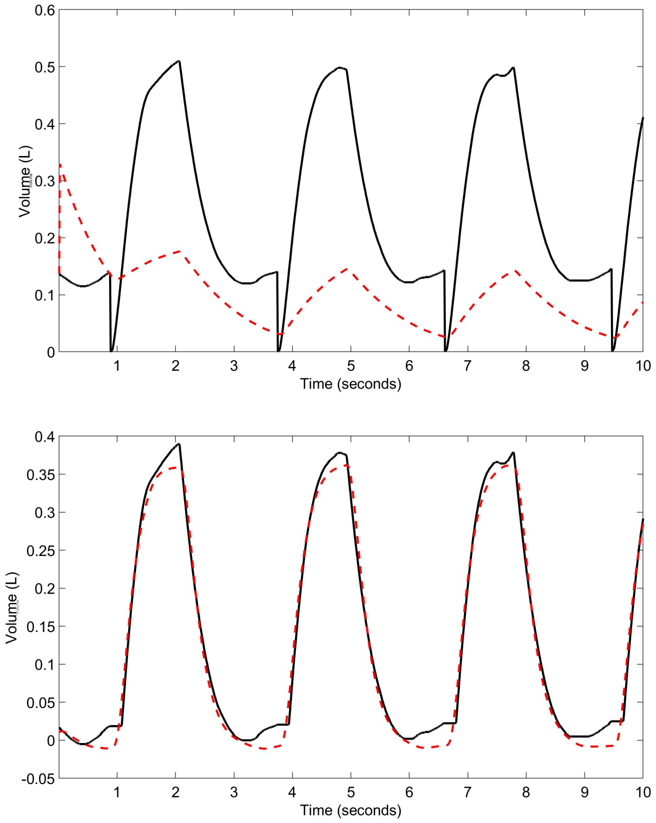

Figure 6.7: Second order linear system of patient 1 with known air leak (expiratory volume is lower than inspiratory volume). This causes the system to be unidentifiable (upper figure). By interpolation of end expiratory phase, the effect of air leak is lifted, resulting in an identifiable system (lower figure).

Results of the second order linear model are shown in table 6.2. The good fit and small SE of parameters suggest that the identified models are able to simulate the system response. A rare case is subject 2 which shows a good fit but a very poor accuracy of estimated parameters. This is an example of the complexity of a second order model. Adding more parameters to a model allows for more degrees of freedom, making it more difficult to get an accurate estimation of parameters. In the first order models, accuracy of parameters and goodness of fit was enough to determine if the model was a good approach of the respiratory system. It is thus important to further analyse characteristics of the identified models to determine if the identified models are indeed a good approach of the respiratory system.

Characteristics of models can be evaluated with poles and zeros. Background information of poles and zeros can be found in Appendix A. The pole and zero map of all identified second order models is shown in figure 6.8. This figure shows that all poles have a negative real part, which means that all systems are stable. The dominant pole - i.e. the part of the system which has the most influence on the system response - are the poles closest to the imaginary axis. These poles determine how fast the system responds, comparable with time constants of the first order linear model. More interestingly, patient 1, 2 and 4 have imaginary poles: the identified models are underdamped. This would mean that by applying an input

Table 6.2: Estimation results of system identification of the second order linear model of the respiratory system. MSE = mean square error. SE = standard error.

Respiratory System					
Subject #	MSE	Fit %	Elastance (SE)	Resistance (SE)	Inertia (SE)
1	2.1^{-04}	90	54 (0.9)	16 (1)	1 (0.06)
2	5.5^{-04}	84	39 (1)	11 (1)	0.8 (0.1)
3	1.0^{-04}	93	23 (2^{+5})	10 (2^{+5})	6^{-04} (2^{+4})
4	6.4^{-04}	81	58 (1)	12 (1)	0.8 (0.09)
5	4.0^{-04}	86	36 (3)	12 (3)	0.6 (0.2)

the respiratory system will oscillate before reaching steady state. The respiratory system then has an eigenfrequency or natural frequency. The natural frequency is the frequency which a system oscillates with when it is moved from an equilibrium position and then released [14]. An example of this phenomenon is seen with a tuning fork; by striking a tuning fork, it will oscillate with a certain frequency. Since the 1950s, oscillatory behaviour of the respiratory system has been studied [21, 22]. This subject however exceeds the scope of this thesis. Notable is that not all identified models show the same characteristics in terms of damped or underdamped. It is possible that the negative end expiratory phase as shown in figure 5.2 has a greater influence in the second order model in comparison with the first order model. Further preprocessing similar to figure 6.7 is needed to accurately identify the respiratory system. It has to be kept in mind that input and output data are heavily influenced by both the human body and mechanical ventilator. The input signal is not a perfect pulse train. Applied pressure is continuously measured during an inspiratory cycle and flow is adapted to try maintain the set pressure. This causes for a noisy input signal and can results in wrongful system identification similar as seen in identification of thorax and lung in chapter 5. In future research, the second order linear model should be further evaluated to determine if and why the system is wrongly identified.

Main findings:

- System identification with transfer functions gives more information about the characteristics of the identified system in comparison with the state space design.
- The time constant is dependent on both elastance and resistance. It is important to be aware of the time constant to understand effects of respiratory frequency on the tidal volume.
- The second order linear model of the respiratory mechanics should be further researched to determine if the respiratory system can be accurately modelled as a second order linear system.

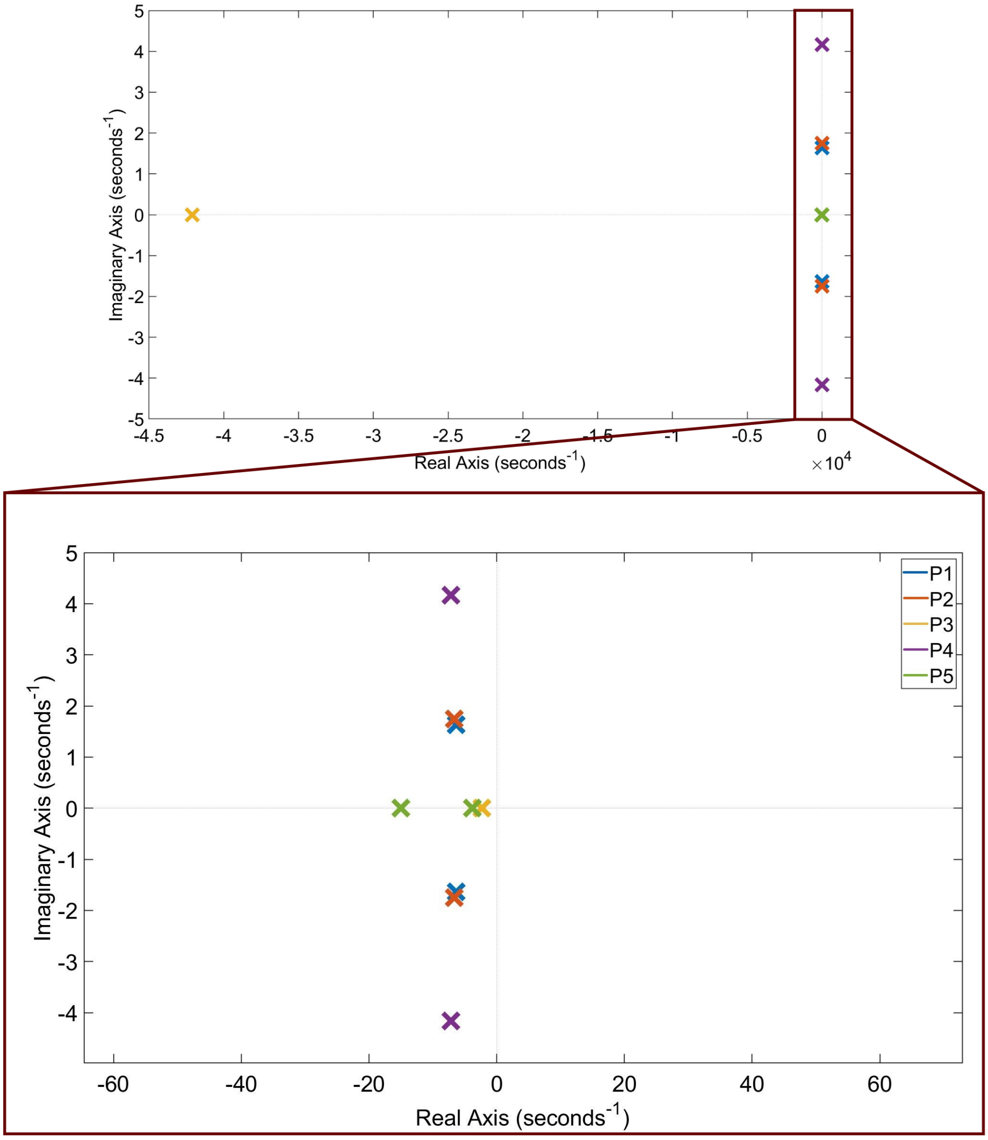

Figure 6.8: Poles and zeros plot of the second order linear model of the respiratory mechanics of the five COVID-19 patients. The second order model has two poles and no zeros. Patient 1, 2 and 4 have imaginary pole indicating that those identified system are underdamped.

Part III

SIMULATION

7 MODEL DESIGN

For educational purposes, it is interesting to visualize the models of the respiratory system and mechanical ventilation for different values of parameters of elastance and resistance in a way that is similar to the clinical setting. The models in this part can also visualize properties of the system which can not be measured in the real system such as alveolar pressure. For simulation of these models MATLAB/Simulink 2019b (Mathworks, Natick, Massachusetts, United States of America) is used. The Simulink models are displayed in Appendix E.

Properties of the mechanical ventilator, resistance and elastance can be manually adapted. In healthy adults, resistance of the respiratory system is between 0.5 and 2 cm H_2O s L^{-1} [9]. For individuals with obstructive diseases, resistance can increase to 15 cm H_2O s L^{-1} [23]. Physiological elastance of the respiratory system is between 4 and 8 cm H_2O L^{-1}. Properties of elastance and resistance in mechanical ventilation are different than in physiological breathing. Resistance is increased up to 10-15 cm H_2O s L^{-1} due to artificial airways needed for mechanical ventilation [24]. In patients with COPD, airway resistance can increase up until 22 cm H_2O s L^{-1} or higher [24]. Elastance also increases to approximately 15-20 cm H_2O L^{-1} in healthy subjects undergoing mechanical ventilation. In restrictive diseases such as ARDS elastance can be increased to 30 and in COPD elastance can be decreased to 13 [24]. Arnal et al. [24] researched typical parameter calues during mechanical ventilation. Results of this study can be used for parameter selection in simulation, table 7.1. Parameter values can also be randomly chosen or estimated parameter values acquired from system identification procedures can be used. V_0 is usually around 2 litres [9].

Table 7.1: (Patho)physiological parameter values of elastance and resistance of the respiratory system in mechanical ventilation for healthy and pathological lung. The parameter values can be used for simulation of respiratory mechanics. From Arnal et al. 2017

Parameter	Healthy Lungs	ARDS	COPD
Elastance	15-23	20-31	13-23
Resistance	10-15	9-14	16-33

7.1 MODEL 1: MODEL OF RESPIRATORY SYSTEM

Most simple model to simulate is the first order linear model as shown in part I. Models in part I describe the relation between pressure difference and volume difference. To simulate this PEEP is set to zero, figure 7.1. The figure shows that alveolar pressure is not equal to airway pressure at the end of inspiration. This can also be seen in the flow curve; the flow is not zero. This indicates that there is still a pressure difference between lung and airway. For clinicians this is important to be aware of since transpulmonary pressure is the resultant of alveolar pressure and pleural pressure. Since alveolar pressure cannot be measured in vivo, an inspiratory or expiratory hold manoeuvre should be done. With these manoeuvres, the valves of the mechanical ventilator are closed to let the flow decay to zero. It is then thought that the pressures measured at the airway are equal to alveolar pressure.

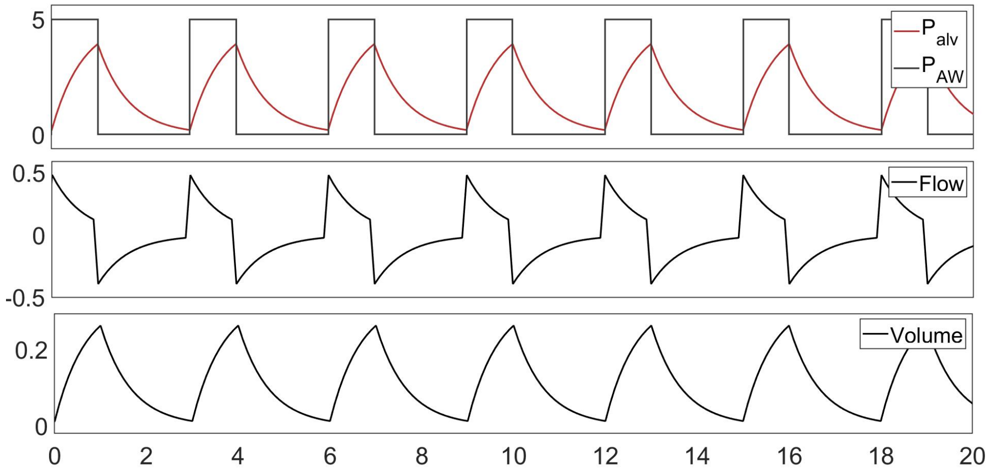

Figure 7.1: Simulation of the first order linear model. To simulate the relation between pressure, flow and volume difference as is done in system identification, PEEP is set to zero. In this example, elastance is 15 cm H_2O L^{-1}, resistance is cm H_2O s L^{-1}. P_{AW} is airway pressure and P_{alv} is alveolar pressure. X-axis represents the time in seconds.

By setting PEEP > 0, the effect of PEEP can be evaluated. By setting PEEP, end expiratory lung volume will not return to zero but is positive, as can be seen in figure 7.2.

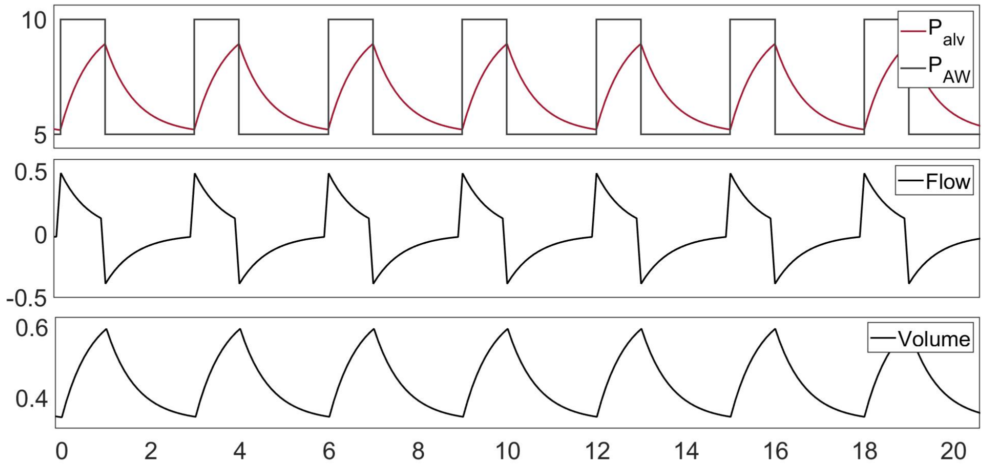

Figure 7.2: Simulation of first order linear model with PEEP. End expiratory lung volume increases to approximately 0.35 L. In this example, elastance is 15 cm H_2O L^{-1}, resistance is cm H_2O s L^{-1}. P_{AW} is airway pressure and P_{alv} is alveolar pressure. X-axis represents time in seconds.

7.2 MODEL 2: MODEL OF THORAX AND LUNG

Model 1 can be expanded with thoracic elastance and lung elastance as separate compartments. With this model pleural pressure and transpulmonary pressure can be visualized as shown in figure 7.2. By increasing PEEP end expiratory lung volume increases. This results to a higher intrathoracic volume and thereby higher pleural pressure. Pleural pressure becomes positive when intrathoracic volume is larger than the resting volume of the thorax (V_{V0_Th}). V_{0_Th} is in physiological cases around 4.6 litres [25].

Summation of thoracic elastance and lung elastance results in elastance of the respiratory system. In healthy individuals elastance of thorax and lung are similar, resulting in an equal distribution of aplied pressure across the two systems. In certain pathologies such as ARDS pressure distribution can be greatly disturbed; thoracic elastance can be up to 4 times smaller or 4 times larger than lung elastance [18]. Thoracic elastance can be increased due to increased body weight, an increase of abdominal pressure by abdominal fluid (ascites) or intestinal distension [18].

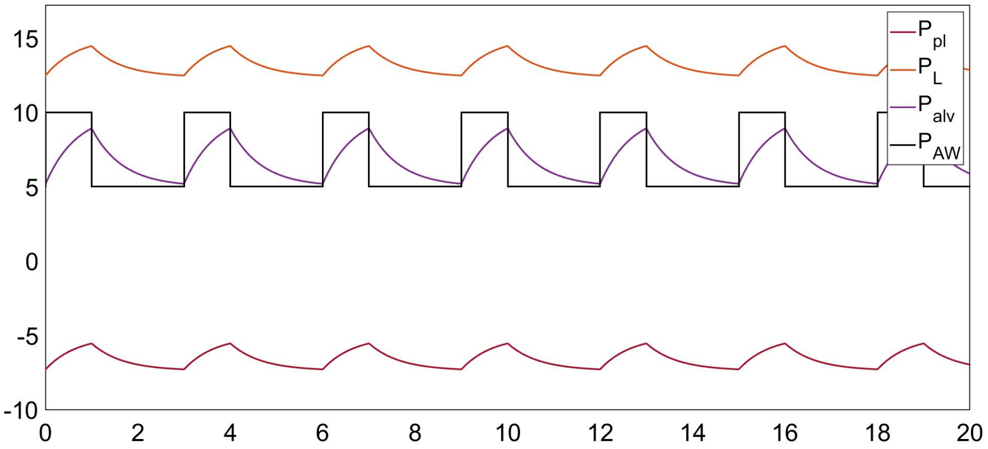

Figure 7.3: Simulation of first order linear model with thoracic and lung elastance. Summation of thorax and lung elastance results in elastance of respiratory system. P_{AW} is airway pressure, P_{alv} is alveolar pressure, P_{pl} is pleural pressure and P_L is transpulmonary pressure. X-axis represents time in seconds.

7.3 MODEL 3: MODEL OF HETEROGENEOUS LUNG

In chapter 2 the concept of heterogeneity is explained. Pathological lungs are often heterogeneous where different lung regions have different elastance and/or resistance values. To simulate this, the lung is divided in to two compartments, equation 7.1:

$$\begin{gathered} P_{AW}(t) = PEEP + E_1 \cdot (V_1 - V_0) + E_2 \cdot (V_2 - V_0) + R_1\dot{V}_1(t) + R_2\dot{V}_2(t) \\ P_{AW}(t) = PEEP + (E_1 + E_2) \cdot (V - V_0) + (R_1 + R_2)\dot{V}(t) \end{gathered} \tag{7.1}$$

From a clinical perspective, it is very interesting to determine local respiratory mechanics. In mechanical ventilation only one volume and one flow is measured. This results in to an infinite amount of possibilities of both the two elastance values and the two resistance values to solve equation 7.1. System identification of this model is therefore insolvable. With simulation however this is not a problem; the observer can manually choose elastance and resistance values of the different compartments. The total lung elastance is a summation of the two individual elastance values of the separate compartments. Resistive components are built in parallel, lowering the total respiratory resistance:

$$\frac{1}{R_{RS}} = \frac{1}{R_1} + \frac{1}{R_2} \tag{7.2}$$

This means that individual resistive components have to be greater when more compartments are set parallel to obtain the same respiratory resistance as used in model 1 or 2. The model allows for the visualisation of volume, flow and pressure for each compartment as well as total flow, volume and pressure, figure 7.4. In this model, it is assumed that pleural pressure is the same across the lung.

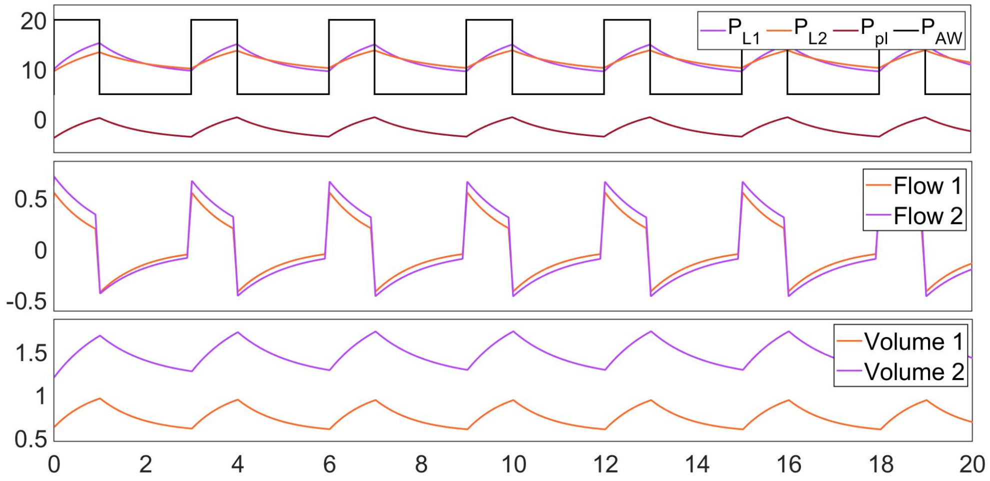

Figure 7.4: Simulation of the two compartment linear model with different resistance and elastance values of separate compartments. Compartment 2 (purple line) has a lower resistance and elastance allowing for more volume. Compartment 1 has less volume due to less flow but has similar transpulmonary pressure caused by the higher elastance in comparison with compartment 2. P_{AW} is airway pressure, P_{pl} is pleural pressure, P_{L1} and P_{L2} are the transpulmonary pressures of the separate compartments. X-axis represents time in seconds.

7.4 MODEL 4: HETEROGENEOUS LUNG WITH RECRUITMENT

The pressure gradient due to gravitational forces and recruitment can be modelled with threshold opening pressures (TOP). When the TOP is reached, elastance of that alveolar compartment changes from a high elastance to a low elastance, allowing inflation and decreasing total lung elastance. Figure 7.5 shows the effect of recruitment on the pressure-volume relation. When the transpulmonary pressure - by an increase of airway pressure or decrease of pleural pressure - of a closed alveolar compartment reached the TOP, the compartment is recruited: the elastance switches from high to low.

The models described above can extended with more compartments to create a more smooth response. Total lung elastance is a summation of all parallel alveolar compartments:

$$E_L = \sum_{i=1}^{n} E_i \tag{7.3}$$

For all parallel respiratory airways, total respiratory resistance can be calculated:

$$R_{RS} = R_{common} + \sum_{i=1}^{n} \frac{1}{R_i} \tag{7.4}$$

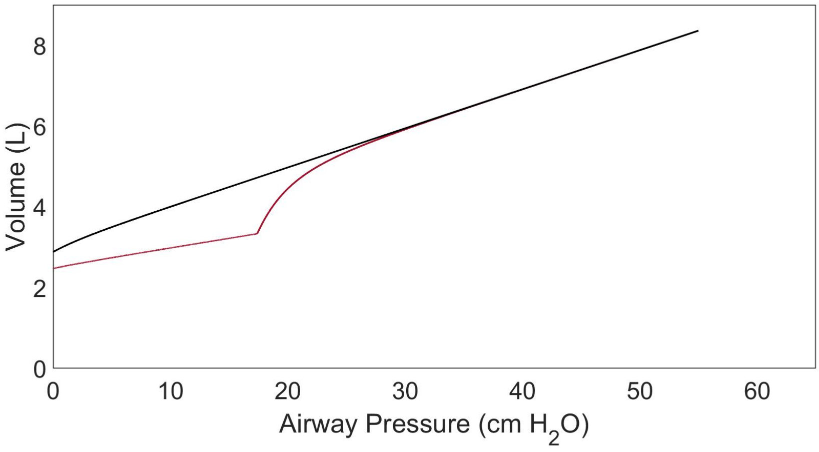

Figure 7.5: Effect of threshold opening pressure (TOP) for pressure-volume relationship in two compartment linear model. The black line represents pressure-volume relationship when both compartments are recruited: a low elastance for all pressures. The red line represents pressure-volume relationship when one compartment has to be recruited through higher pressures. Before recruitment, total respiratory elastance is low. When the second compartment is recruited, this compartment contributes to the ventilation thereby decreasing the total respiratory elastance.

Part IV

FUTURE IMPLICATIONS

8 FUTURE IMPLICATIONS

8.1 FUTURE RESEARCH

This thesis gives an overview of the most important respiratory mechanics and modelling of these respiratory mechanics. Even though the models described in this thesis have been extensively researched and applied [9, 11, 26], system identification of these models have shown there is still a need for further research. This can be explained by the input and output signals used for system identification, which need more prepocessing and/ or filtering. As discussed before, oesophageal pressure curves need additional preprocessing in the form of filtering of cardiac noise to allow for accurate estimation of parameters. It is also possible to use system identification techniques which encounter for noisy input signals. Additional preprocessing might also benefit system identification of the second order linear model.

Chapter 5 has shown the first order linear model as an accurate representation of the respiratory system. This conclusion is drawn from validation of five patients with the same pathology, mostly showing restrictive respiratory mechanics. To further validate the model, it should be evaluated if different types of pulmonary diseases with different respiratory mechanics can also be accurately identified. The database should at least include healthy lungs, additional restrictive diseases such as lung fibrosis and pulmonary oedema and obstructive diseases such as asthma and COPD. All these patients are part of the ICU population which receive mechanical ventilation and should therefore be included in further application of the models.

After further validation, the models can be used to perform in silico studies. A possible application can be to research the optimal ventilation settings in controlled mechanical ventilation. In 2016 Gattinoni et al. [27] proposed mechanical power as a parameter directly correlated with VILI. This mechanical power describes the energy that is applied to the respiratory system by the mechanical ventilator. The last years the hypothesis has arisen that the mechanical power should be minimised. The first order linear model can help to understand and determine optimal ventilation settings by limiting mechanical power given a set minute volume. It is also possible that the pressure wave forms in pressure controlled ventilation are not the ideal wave form to minimise mechanical power. With the use of the models, other waves forms can be explored to optimise ventilation strategies.

8.2 FURTHER MODEL DEVELOPMENT

In chapter 2 it is discussed that the respiratory system behaves as a nonlinear system. Because the first order linear model shows good accuracy, it is most likely that nonlinear behaviour is small during the range of pressures used in mechanical ventilation. From a clinical perspective, it is interesting to research if nonlinear behaviour is present when there are setting changes applied to mechanical ventilation. It is expected that for example a change of PEEP leads to a change in elastance which is important to evaluate for lung protective ventilation. This possible nonlinear behaviour makes it difficult to predict the result of ventilator setting changes at bedside. By identification of nonlinear behaviour in models, it might be possible for clinicians to get better in predicting effects of ventilator settings. The expectation is that more insight will lead to more lung protective ventilation with better patient outcomes. To explore possible nonlinear behaviour with system identification, input signals should include changes in ventilator settings. If the linear model is still an accurate representation of the system, nonlinear behaviour is negligible. If not, the role of non-linearity can be explored. This can be done by approaching the system as a black box - i.e. with no prior knowledge of the structure of the system, with the use of so called Volterra series [15]. With this approach, parameters of the system are not estimated, but rather parameters of linear and nonlinear components between input and output. Parameters describing non linearity gives an indication of the magnitude of nonlinear behaviour.

In mechanical ventilation, respiratory mechanics are not the only aspect that should be understood and encountered for in the clinical setting. The respiratory mechanics influence gas exchange and hemodynamics of an individual. A complete image of the effects of mechanical ventilation should therefore include the respiratory mechanics, gas exchange and hemodynamics. The ventilation is set in such a way that is beneficial for lung protective ventilation but has negative effects on gas exchange or hemodynamics of the patient. The understanding of the interaction between respiratory mechanics, gas exchange and hemodynamics is thus of great importance for adequate treatment of patients.

The respiratory mechanics are much more complex than described in this thesis. For example, nonlinear resistance, time dependent recruitment and derecruitment are not discussed. However, it is important to evaluate if more complexity leads to a more accurate model. As shown in chapter 6 introduction of more complexities such as from a first order model to a second order model, will introduce extra difficulties. The level of complexity for system identification will be limited. For simulation, there are not really limitations to the complexity of the models that can be made. It is however difficult to evaluate the accuracy of these models. Without system identification, the structure of the system will be theoretical and cannot be validated with experimental data.

BIBLIOGRAPHY

1. Vesalius, A. *De humani corporis fabirca* (1543).
2. Slutsky, A. S. History of Mechanical Ventilation. From Vesalius to Ventilator-induced Lung Injury. *American Journal of Respiratory and Critical Care Medicine* **191,** 1106–1115 (2015).
3. Boron, W. F. & Boulpaep, E. L. *Medical Physiology: A cellular and molecular approach* (Saunders/Elsevier, Philadelphia, PA).
4. Van IJzendoorn M Koopmans M, S. U. e. a. Ventilator settings in ICUs: comparing a Dutch with a global cohort.
5. Mead J Takishima T, L. D. Stress distribution in lungs: a model of pulmonary elasticity. *Journal of Applied Physiology* **28,** 596–608 (1970).
6. The Acute Respiratory Distress Syndrome Network. Ventilation with Lower Tidal Volumes as Compared with Traditional Tidal Volumes for Acute Lung Injury and the Acute Respiratory Distress Syndrome. *The New England Journal of Medicine* **342,** 1301–1308 (2000).
7. Otis, A. B. *et al.* Mechanical Factors in Distribution of Pulmonary Ventilation. *Journal of Applied Physiology* **8,** 427–443 (1956).
8. Ljung, L. *System Identification - Theory For the User* (Prentice Hall PTR, 1999).
9. Maury, B. *The Respiratory System in Equations* (Springer-Verlag Italia, 2013).
10. Gattinoni, L., Carlesso, E. & Caironi, P. Stress and strain within the lung. *Current Opinion in Critical Care* **18,** 42–47 (2012).
11. Bates, J. *Lung Mechanics: An Inverse Modeling Approach* (Cambridge Univeristy Press, New York, 2009).
12. Mead J Whittenberger JL, R. E. J. Surface tension as a factor in pulmonary volume-pressure hysteresis. *Journal of Applied Physiology* **10,** 191–196 (1957).
13. Westwick, D. T. & Kearney, R. E. *Identification of Nonlinear Physiological Systems* ISBN: 9780471722960 (John Wiley Sons, Ltd, 2005).
14. Franklin, G. F., Powell, D. J. & Emami-Naeini, A. *Feedback Control of Dynamic Systems* 7th (Prentice Hall PTR, USA, 2015).
15. Åström, K. J. & Murray, R. M. *Feedback Systems: An Introduction for Scientists and Engineers* (2004).
16. Yoshida, T. *et al.* Esophageal Manometry and Regional Transpulmonary Pressure in Lung Injury. *American Journal of Respiratory and Critical Care Medicine* **197,** 1018–1026 (2018).
17. Akoumianaki, E. *et al.* The Application of Esophageal Pressure Measurement in Patients with Respiratory Failure. *American Journal of Respiratory and Critical Care Medicine* **189,** 520–531 (2014).
18. Gattinoni, L., Chiumello, D., Carlesso, E. & Valenza, F. Bench-to-bedside review: Chest wall elastance in acute lung injury/acute respiratory distress syndrome patients. *Critical care (London, England)* **8,** 350–5 (Nov. 2004).
19. Pelosi, P. *et al.* Effects of the Prone Position on Respiratory Mechanics and Gas Exchange during Acute Lung Injury. *American Journal of Respiratory and Critical Care Medicine* **157,** 387–393 (1998).
20. Van der Zee, P., Somhorst, P., Endeman, H. & Gommers, D. Electrical Impedance Tomography for Positive End-Expiratory Pressure Titration in COVID-19–related Acute Respiratory Distress Syndrome. *American Journal of Respiratory and Critical Care Medicine* **202,** 280–284 (2020).

21. Mead, J. Measurement of Inertia of the Lungs at Increased Ambient Pressure. *Journal of Applied Physiology* **9.** PMID: 13376430, 208–212 (1956).

22. Kaczka, D. & Dellaca, R. L. Oscillation Mechanics of the Respiratory System: Applications to Lung Disease. *Critical Reviewstrade; in Biomedical Engineering* **39,** 337–359. ISSN: 0278-940X (2011).

23. Ritz, T. *et al.* Guidelines for mechanical lung function measurements in psychophysiology. *Psychophysiology* **39,** 546–567 (2002).

24. Arnal, J.-M., Garnero, A., Saoli, M. & Chatburn, R. L. Parameters for Simulation of Adult Patients During Mechanical Ventilation. *Respiratory Care* (2017).

25. Rahn, H., Otis, A. B., Chadwick, L. E. & Fenn, W. O. The Pressure-Volume Diagram of the Thorax and Lung. *American Journal of Physiology-Legacy Content* **146,** 161–178 (1946).

26. Das, A. *et al.* Development of an integrated model of cardiovascular and pulmonary physiology for the evaluation of mechanical ventilation strategies. *Conference proceedings : Annual International Conference of the IEEE Engineering in Medicine and Biology Society. IEEE Engineering in Medicine and Biology Society. Annual Conference* **2015,** 5319—5322. ISSN: 1557-170X (2015).

27. Gattinoni, L., Tonetti, T. & Cressoni, M. Ventilator-related causes of lung injury: the mechanical power. *Intensive Care Medicine* **42,** 01567–1575 (2016).

Part V

APPENDICES

APPENDIX A: LAPLACE TRANSFORM, BODE PLOT AND POLES AND ZEROS

LAPLACE TRANSFORM

The Laplace transform is an integral transform that transforms a signal to the s-domain which is a complex variable with a real part σ and a complex part jω.

$$\mathrm{F(s)} = \int_0^\infty f(t)e^{-st}dt$$
$$\text{where } \mathrm{s} = \sigma + \mathrm{j}\omega$$

The Laplace transform is a mathematical tool which allows for transforming differential equations in to algebraic equations. For example, differentiation becomes multiplication and integration becomes division. The Laplace transform is convenient in system identification; it allows for analysis of characteristics of the system both for transient response as for steady state response.

BODE PLOT

The frequency response of a system can be found by substituting s with jω:

$$\mathrm{G(s)} = \frac{1}{\mathrm{s + k}} \rightarrow \mathrm{G(j}\omega) = \frac{1}{\mathrm{j}\omega + \mathrm{k}}$$

With this, magnitude and phase of the system as response to a sinusoidal input signal with frequency ω:

$$\mathrm{M} = \left|\frac{1}{\mathrm{j}\omega + \mathrm{k}}\right| \text{ and } \phi = -\tan^{-1}\left(\frac{\omega}{\mathrm{k}}\right)$$

The magnitude is essentially the amplitude ratio between input and output value. A negative magnitude indicates that the amplitude of the input signal is reduced. A positive magnitude indicates that the amplitude of the input is signal is increased. Magnitude and phase difference between input and output is shown in the figure below. The output is half the input amplitude, which means that the magnitude M is -2. A full sinusoidal phase is 360 degrees. The output is a quarter of a phase behind, which means that the phase is -90 degrees. A negative phase means that the output signal lags the input signal. The Bode plot visualizes magnitude and phase for different frequencies [14].

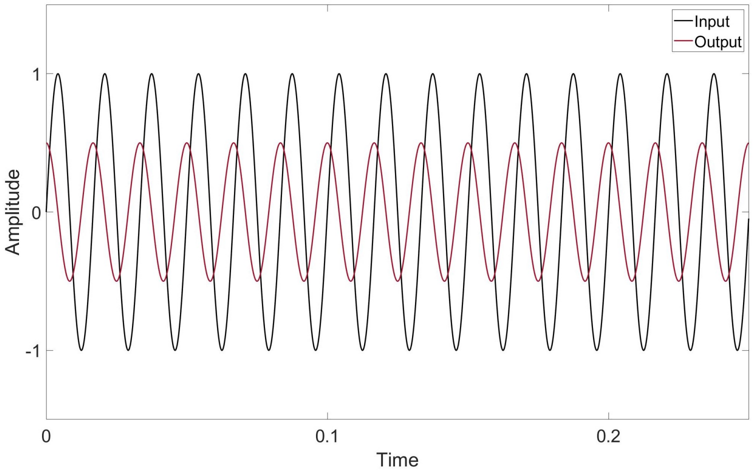

Visualisation between magnitude and phase difference between input (black) and output (red). The magnitude is -2 meaning that the amplitude of the input is reduced with a factor 2. The output is a quarter phase behind the input signal, which corresponds with a phase difference of -90.

POLES AND ZEROS

The poles and zeros of a system characterise its behaviour. The poles (p) can be deduced from the denominator and the zeros (z) from the numerator of the transfer function:

$$G(s) = \frac{s \;- z}{s \;- p}$$

Zeros are found by setting the numerator equal to zero and then solving the equation for s. This is repeated for the denominator to find the poles. The following example contains one zero at s = -2 and two poles at s = -2 and s = -3:

$$G(s) = \frac{s{+}1}{s^2 + 5s + 6} = \frac{s{+}1}{(s + 3)(s + 2)}$$

$$\text{zero} \rightarrow s + 1 = 0 \rightarrow s = -1$$
$$\text{poles} \rightarrow (s + 3)(s + 2) = 0 \rightarrow s = -3,\ s = -2$$

Poles and zeros can be plotted in the s-plane. The locations of poles and zeros in this plane give insight in the response characteristics. A pole location is indicated with a cross, ×. The influence of the pole location is shown in the figure below. The two imaginary poles are complex conjugates; the positive and negative imaginary part are equal to cancel each other out since the system is real valued. If the real part of a pole is negative, the system is stable meaning that it reaches steady state. If the real part of a pole is positive, the system is called unstable meaning that the system does not reach steady state. When the poles are imaginary with either a negative or a positive real part, the systems response is underdamped resulting in oscillations. The location of zeros is a little more complicated. A zero close to a pole location reduces the influence of that pole on the output response. The effect of a zero on the system response is thus dependent on its relation to a pole. [14].

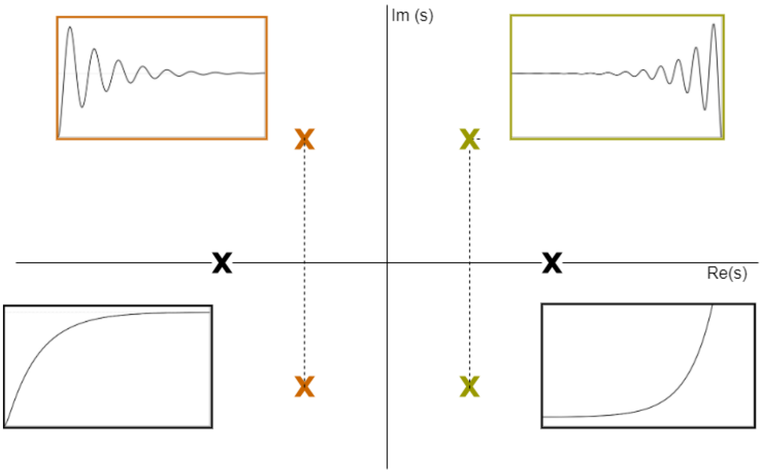

The influence of pole locations on time functions. A stable system has its poles on the negative part of the real axis. When the poles are imaginary with either a negative or a positive real part, the systems response is underdamped. An imaginary pole is a complex conjugate: for a real value the imaginary part is equal negative and positive.

APPENDIX B: MEASURED PATIENT DATA AND PREPROCESSING

Patient data files were extracted from the mechanical ventilation and preprocessed for system identification. Airway pressure (P_{AW}), flow, volume and oesophageal pressure P_{es} curves were directly extracted from the mechanical ventilator. Transpulmonary pressure curves (P_L) were acquired by subtracting the oesophageal pressure from the airway pressure: P_L = P_{AW} - P_{es}. The raw data includes artefacts, changes in mechanical ventilation settings and drifts of the pressure curves mainly from P_{es}. For system identification, a time frame was cut from raw data. This time frame contains a stable signal without any artefacts. To increase accuracy of the model, the time frame is as long as possible. To acquire pressure differences as an input, resting pressure (P_0) is subtracted from the pressure curves. From the time frame a single inspiratory leg is extracted for system identification using the step experiment. The input of the step response is the unit step function which has an amplitude of 1. The step response should therefore be normalised; the step response is divided by the pressure difference of P_{AW}. Results of raw and preprocessed data of each patient are shown below.

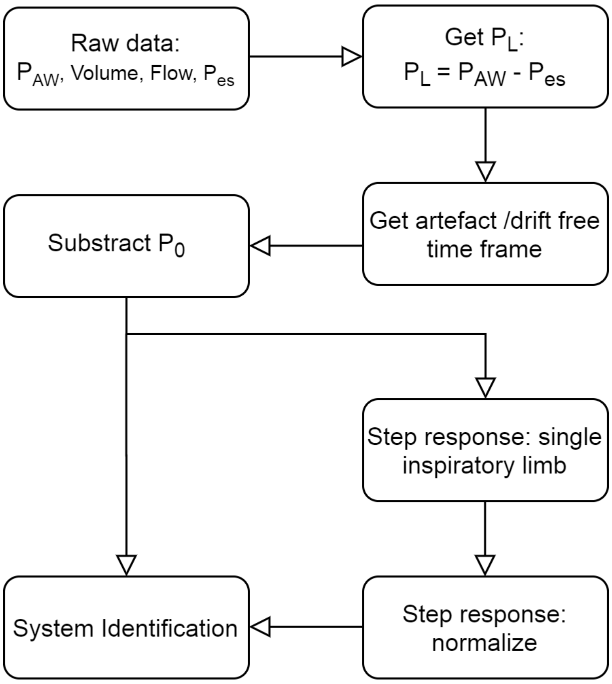
Raw data:
P_AW, Volume, Flow, P_es
Get P_L:
P_L = P_AW - P_es
Get artefact /drift free time frame
Substract P_0
Step response: single inspiratory limb
Step response: normalize
System Identification

Flowchart of preprocessing steps for system identification.

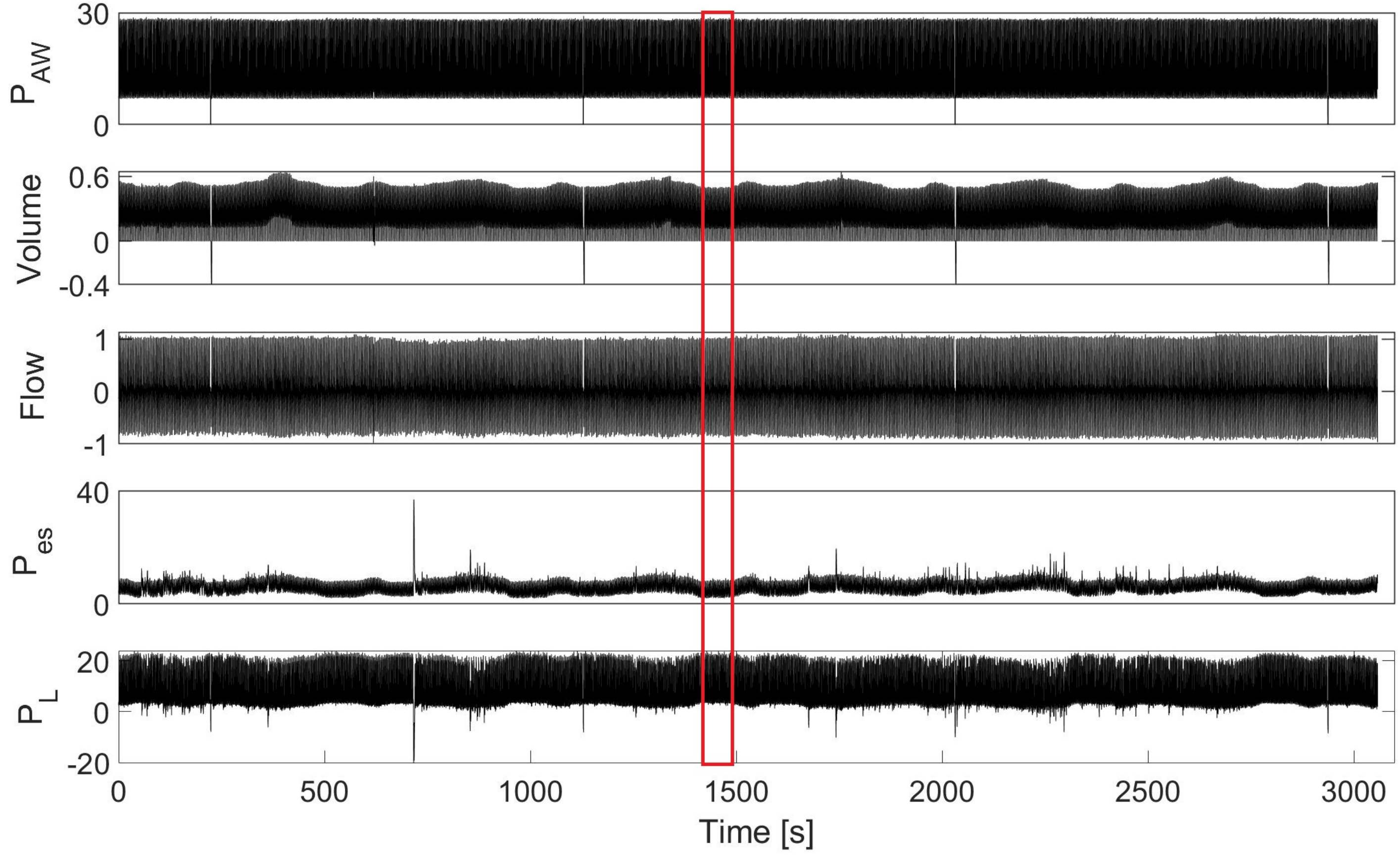

Raw data extracted from the mechanical ventilator for patient 1. The red box is the data frame used for system identification. P_{AW} is airway pressure, P_{es} is oesophageal pressure and P_L is transpulmonary pressure. P_{AW}, P_{es} and P_L are in cm H_2O. Volume is in L and flow in L s^{-1}.

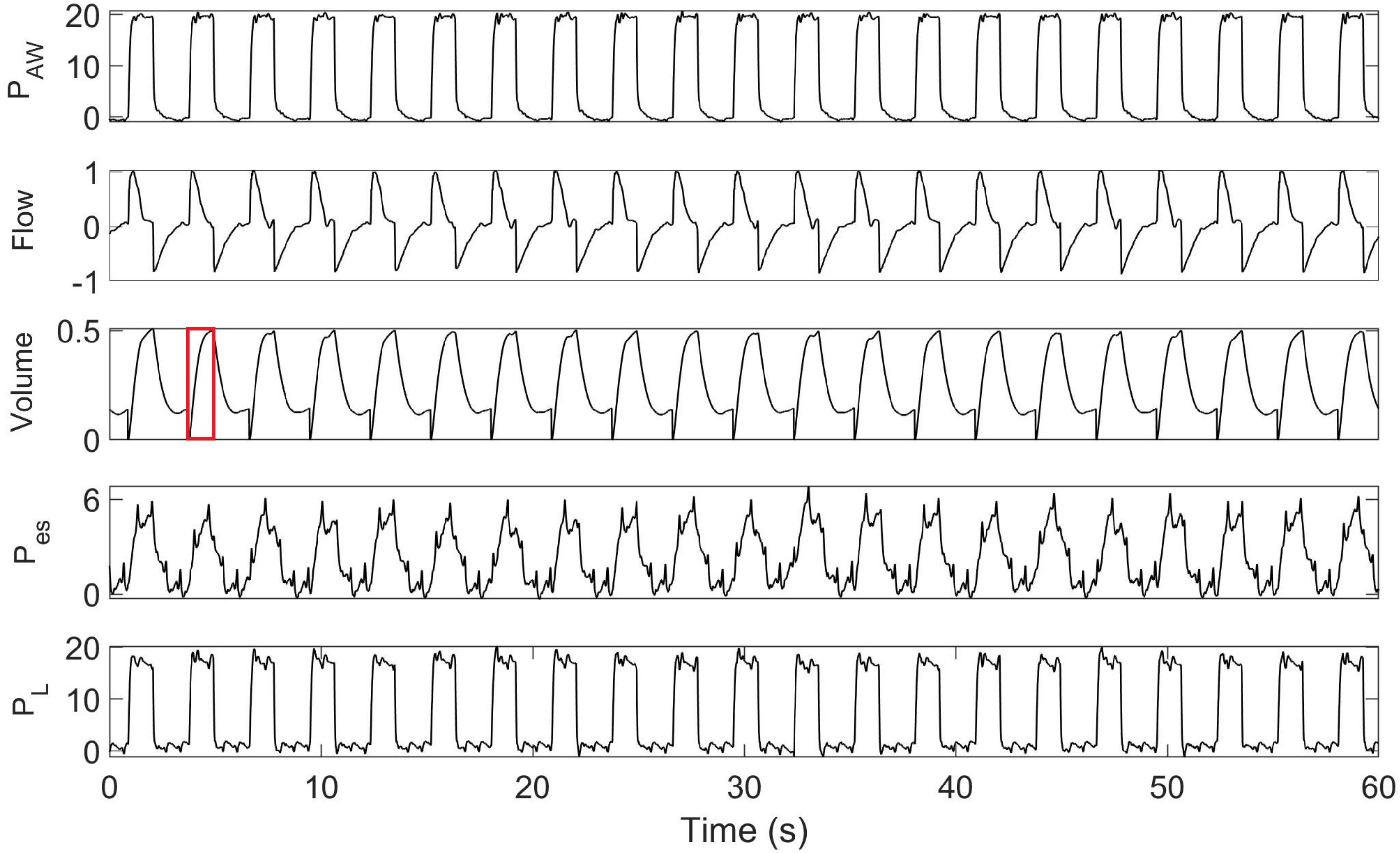

Preprocessed data of patient 1 used for system identification. The red box is the data frame used for system identification with the step experiment. P_{AW} is airway pressure, P_{es} is oesophageal pressure and P_L is transpulmonary pressure. P_{AW}, P_{es} and P_L are in cm H_2O. Volume is in L and flow in L s^{-1}.

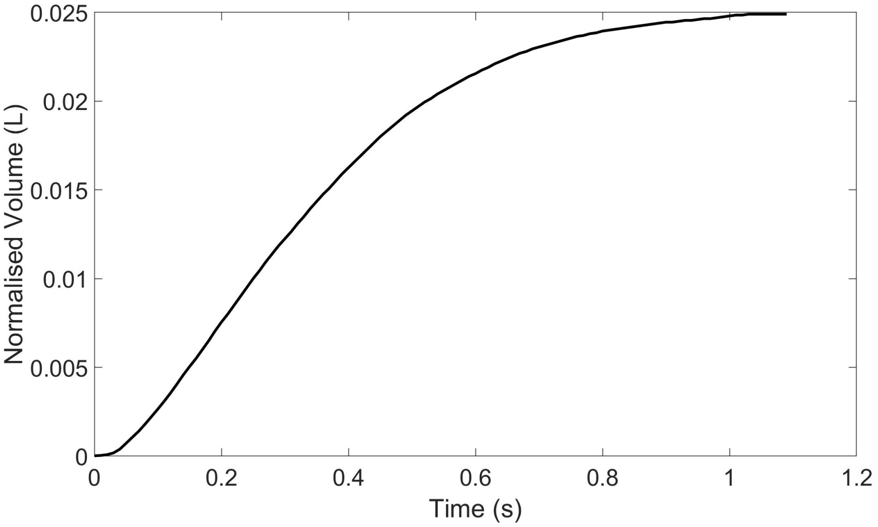

Single inspiratory leg of a breath used for system identification using the step experiment. The volume curve is normalised by dividing the signal with the pressure difference of airway pressure.

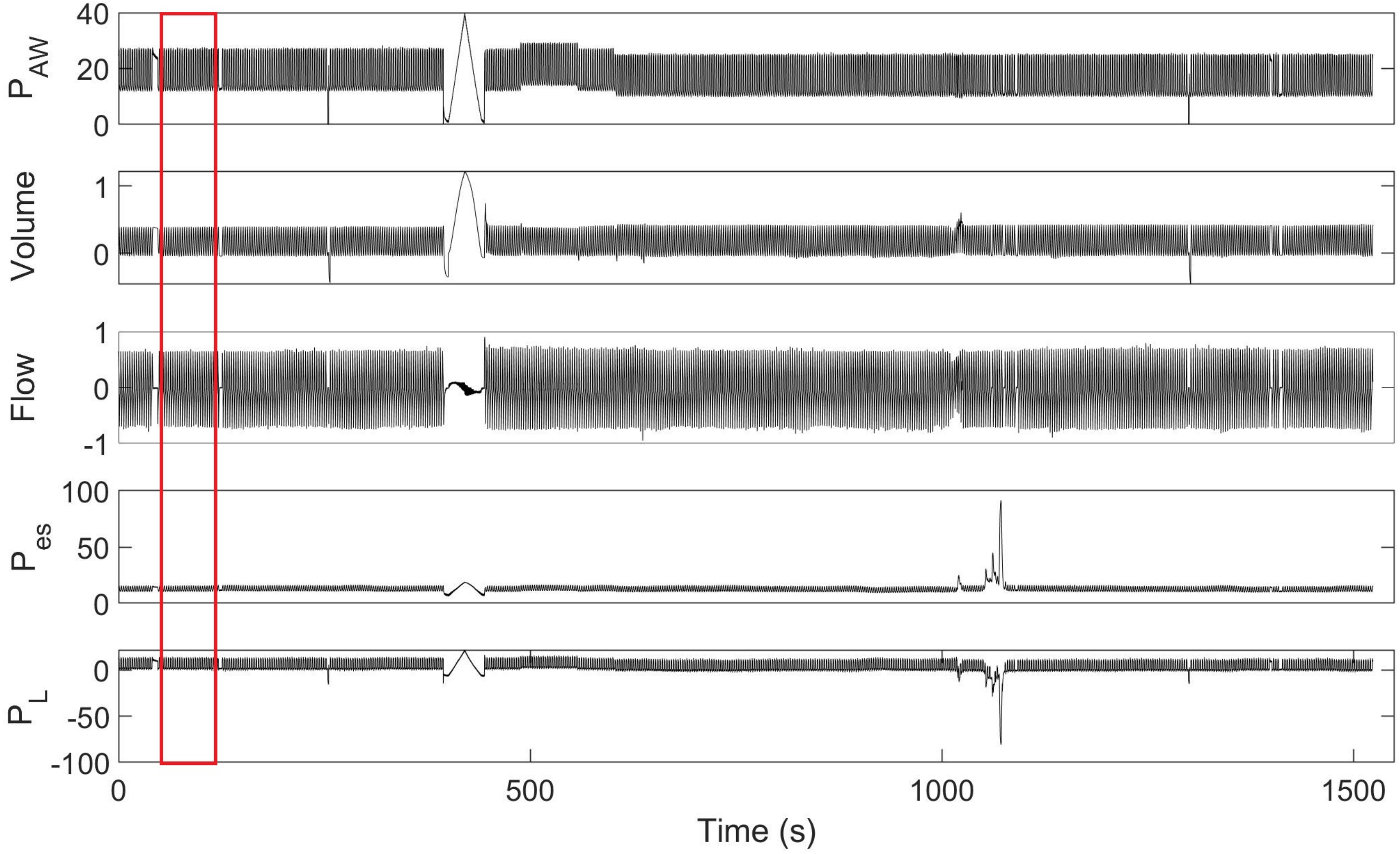

Raw data extracted from the mechanical ventilator for patient 2. The red box is the data frame used for system identification. P_{AW} is airway pressure, P_{es} is oesophageal pressure and P_L is transpulmonary pressure. P_{AW}, P_{es} and P_L are in cm H_2O. Volume is in L and flow in L s^{-1}.

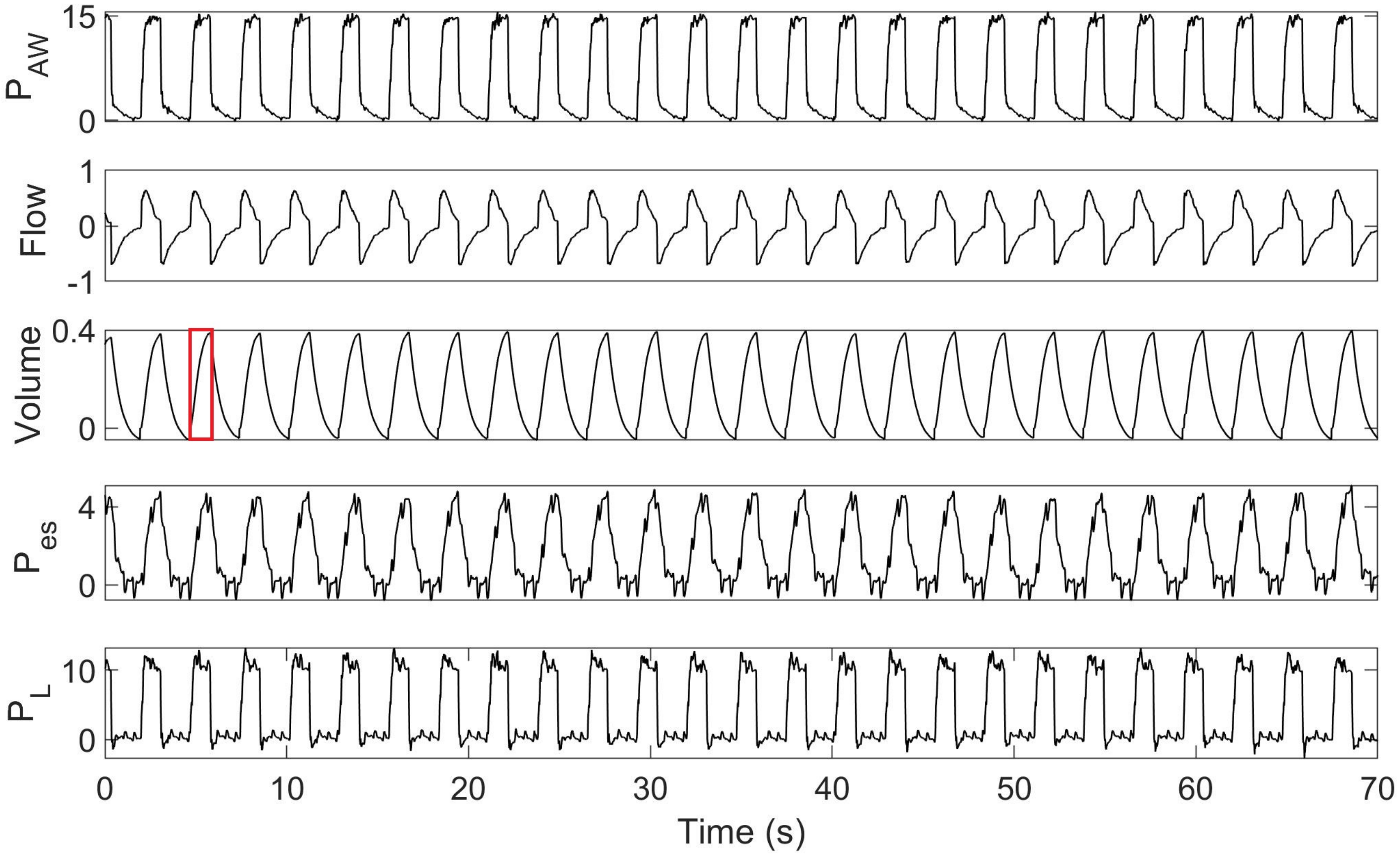

Preprocessed data of patient 2 used for system identification. The red box is the data frame used for system identification with the step experiment. P_{AW} is airway pressure, P_{es} is oesophageal pressure and P_L is transpulmonary pressure. P_{AW}, P_{es} and P_L are in cm H_2O. Volume is in L and flow in L s^{-1}.

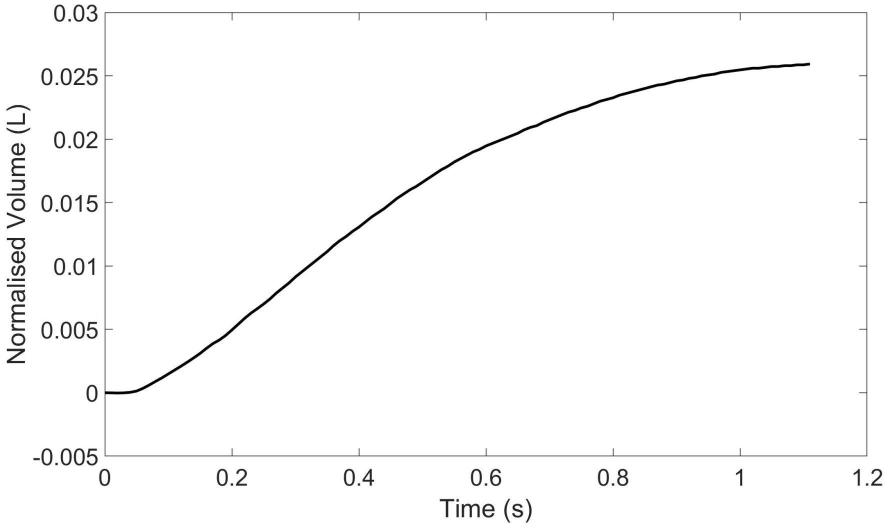

Single inspiratory leg of a breath used for system identification using the step experiment. The volume curve is normalised by dividing the signal with the pressure difference of airway pressure.

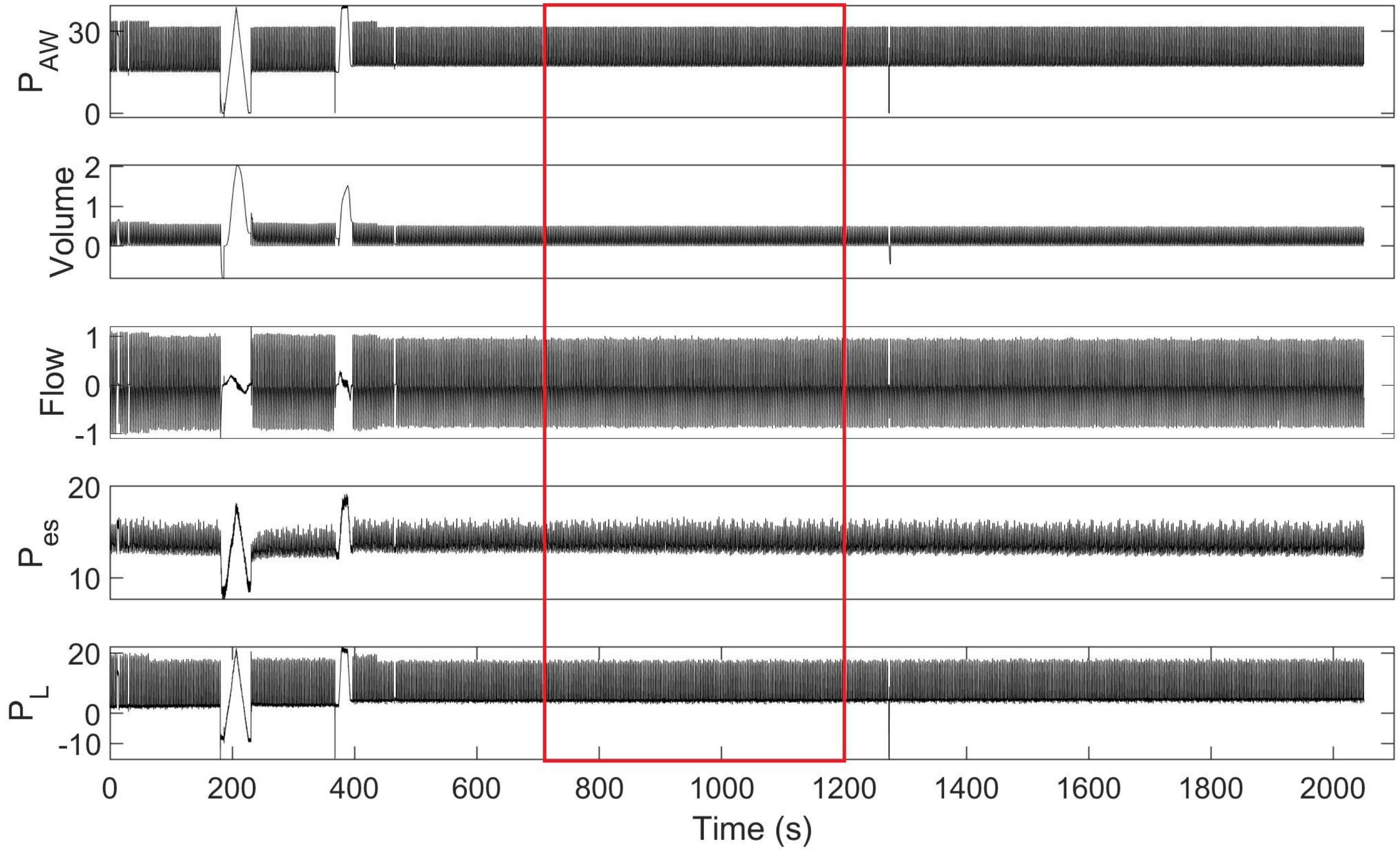

Raw data extracted from the mechanical ventilator for patient 3. The red box is the data frame used for system identification. P_{AW} is airway pressure, P_{es} is oesophageal pressure and P_L is transpulmonary pressure. P_{AW}, P_{es} and P_L are in cm H_2O. Volume is in L and flow in L s^{-1}.

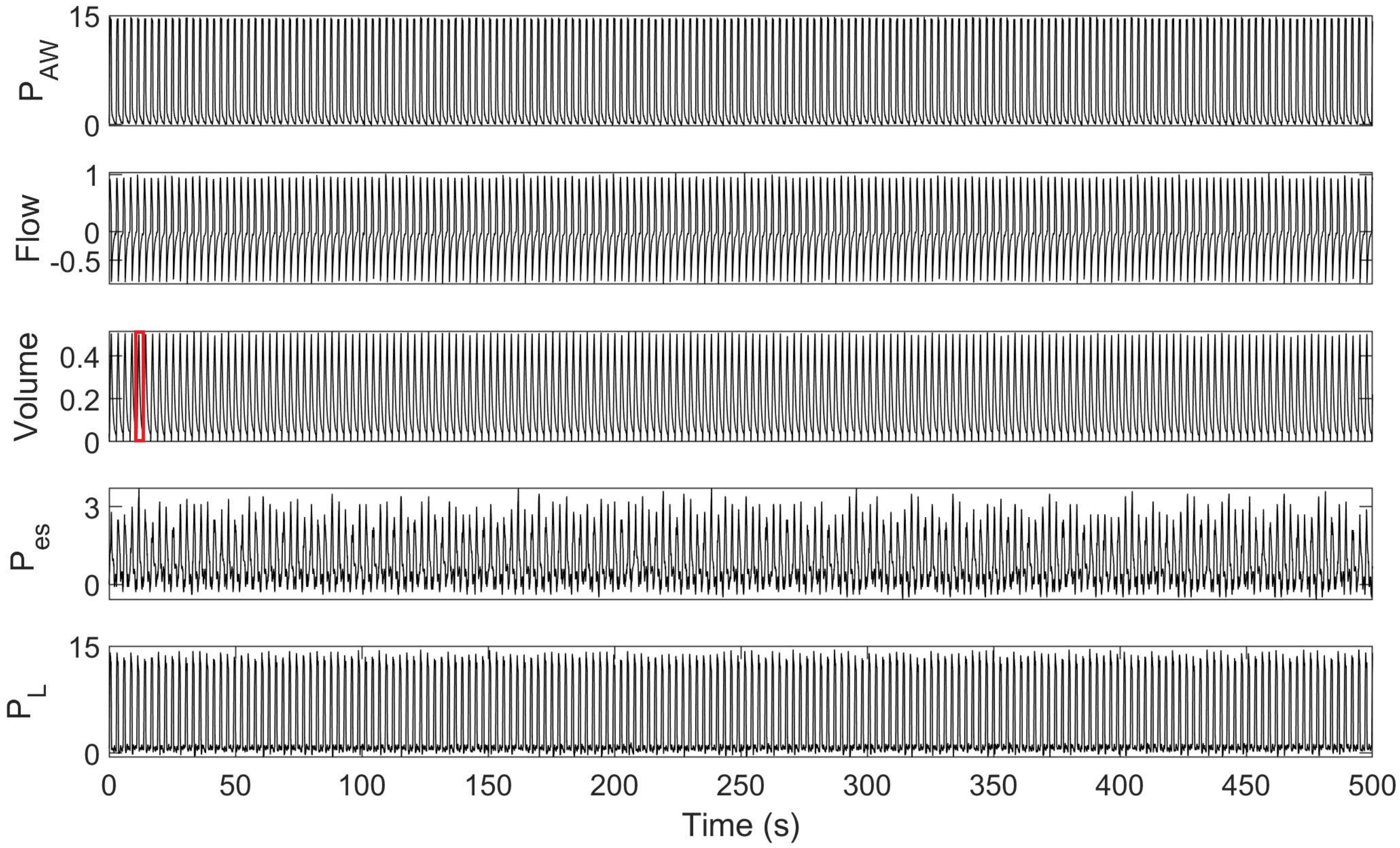

Preprocessed data of patient 3 used for system identification. The red box is the data frame used for system identification with the step experiment. P_{AW} is airway pressure, P_{es} is oesophageal pressure and P_L is transpulmonary pressure. P_{AW}, P_{es} and P_L are in cm H_2O. Volume is in L and flow in L s^{-1}.

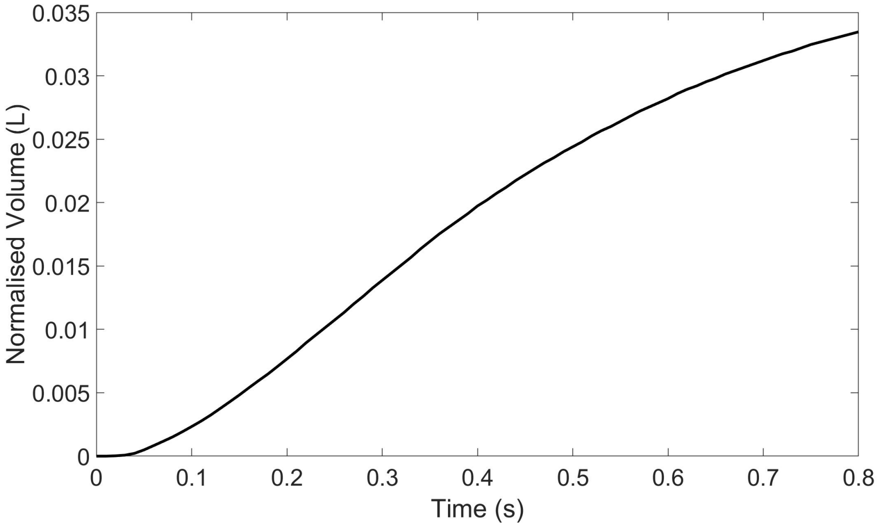

Single inspiratory leg of a breath used for system identification using the step experiment. The volume curve is normalised by dividing the signal with the pressure difference of airway pressure.

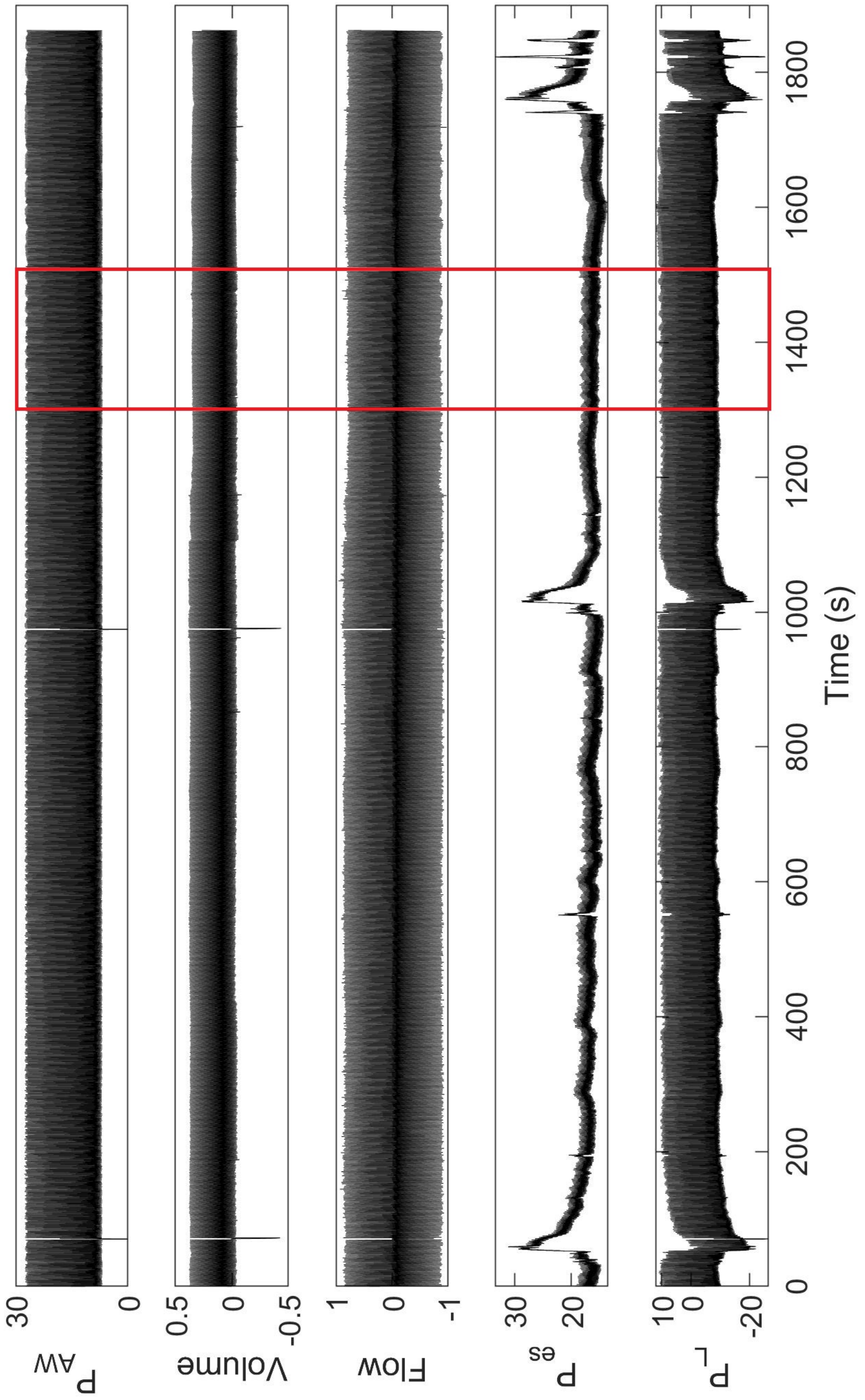

Raw data extracted from the mechanical ventilator for patient 4. The red box is the data frame used for system identification. P_{AW} is airway pressure, P_{es} is oesophageal pressure and P_L is transpulmonary pressure. P_{AW}, P_{es} and P_L are in cm H_2O. Volume is in L and flow in L s^{-1}.

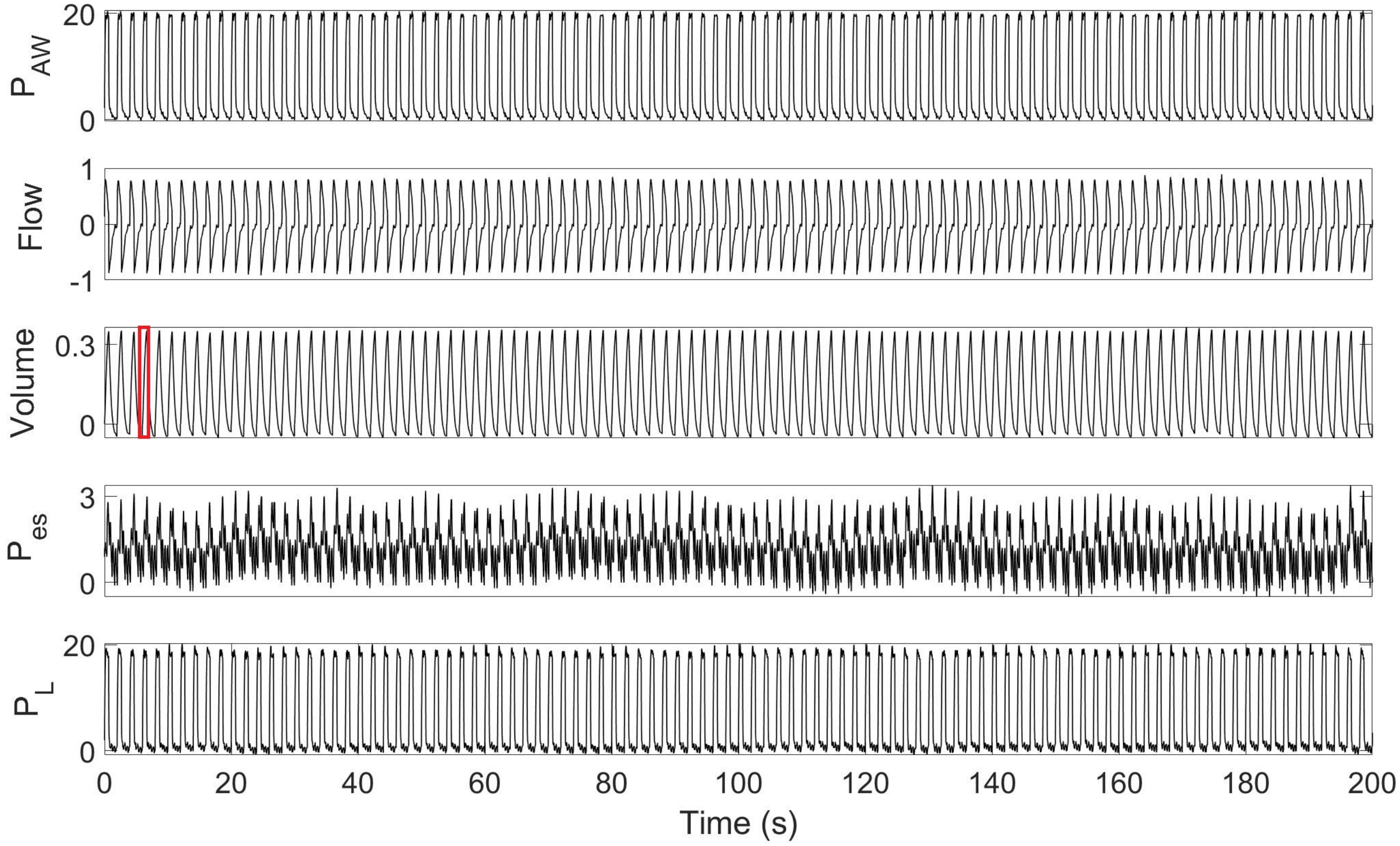

Preprocessed data of patient 4 used for system identification. The red box is the data frame used for system identification with the step experiment. P_{AW} is airway pressure, P_{es} is oesophageal pressure and P_L is transpulmonary pressure. P_{AW}, P_{es} and P_L are in cm H_2O. Volume is in L and flow in L s^{-1}.

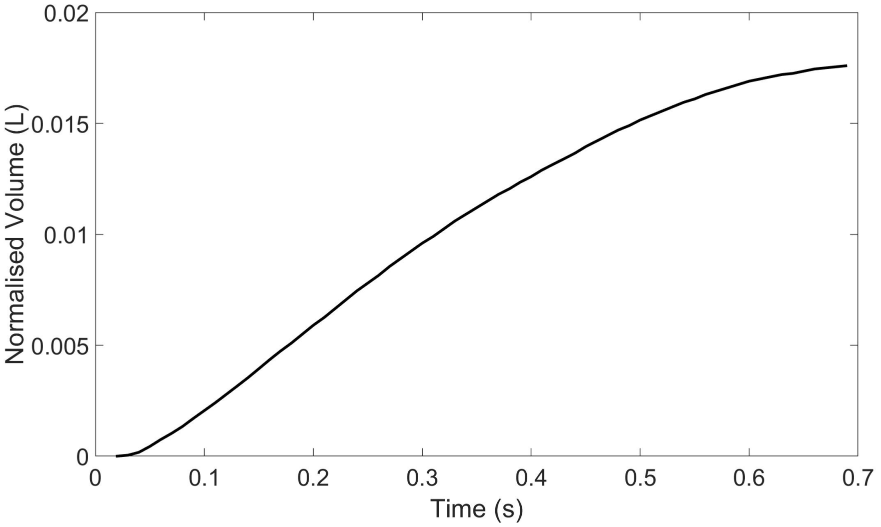

Single inspiratory leg of a breath used for system identification using the step experiment. The volume curve is normalised by dividing the signal with the pressure difference of airway pressure.

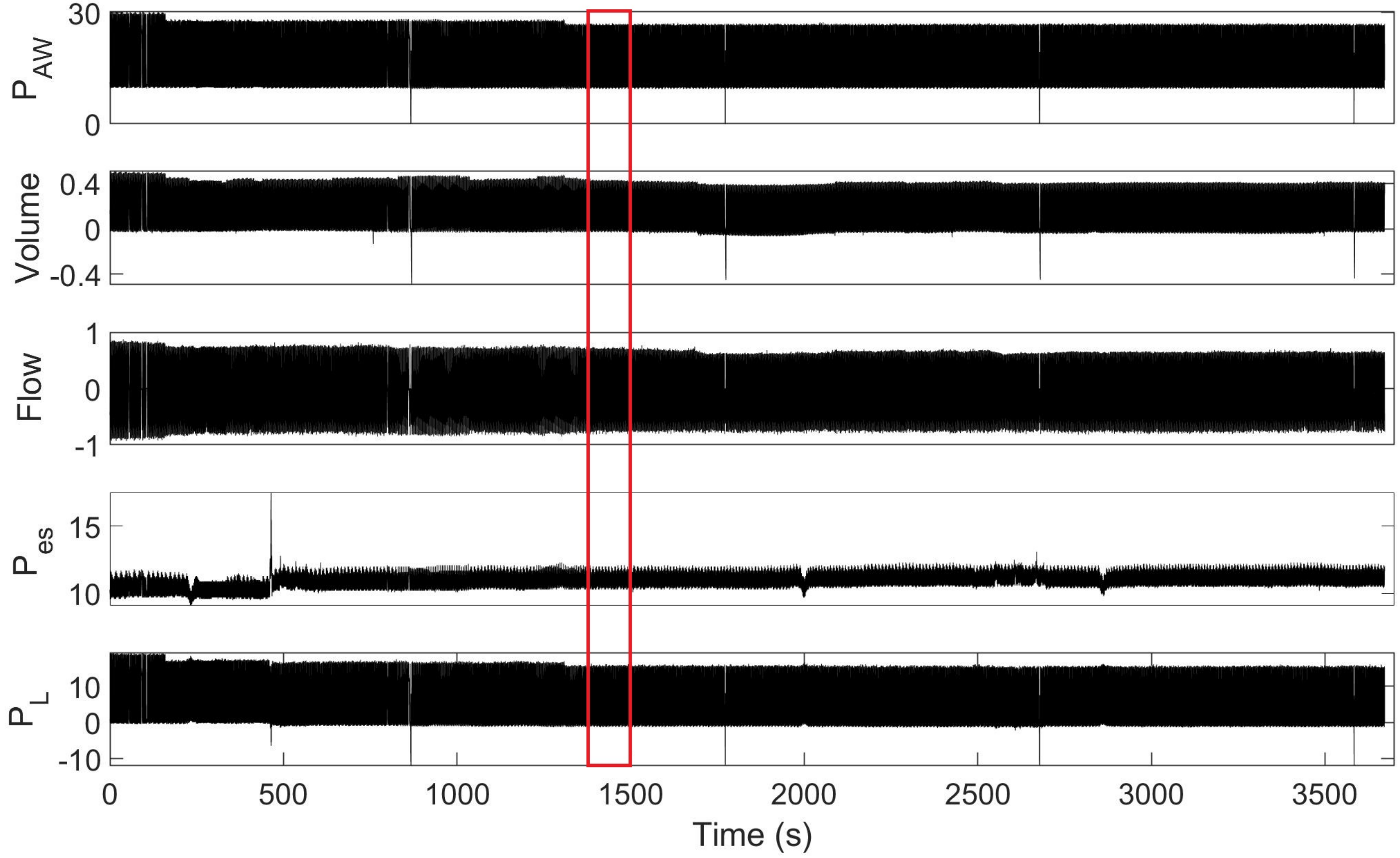

Raw data extracted from the mechanical ventilator for patient 5. The red box is the data frame used for system identification. P_{AW} is airway pressure, P_{es} is oesophageal pressure and P_L is transpulmonary pressure. P_{AW}, P_{es} and P_L are in cm H_2O. Volume is in L and flow in L s^{-1}.

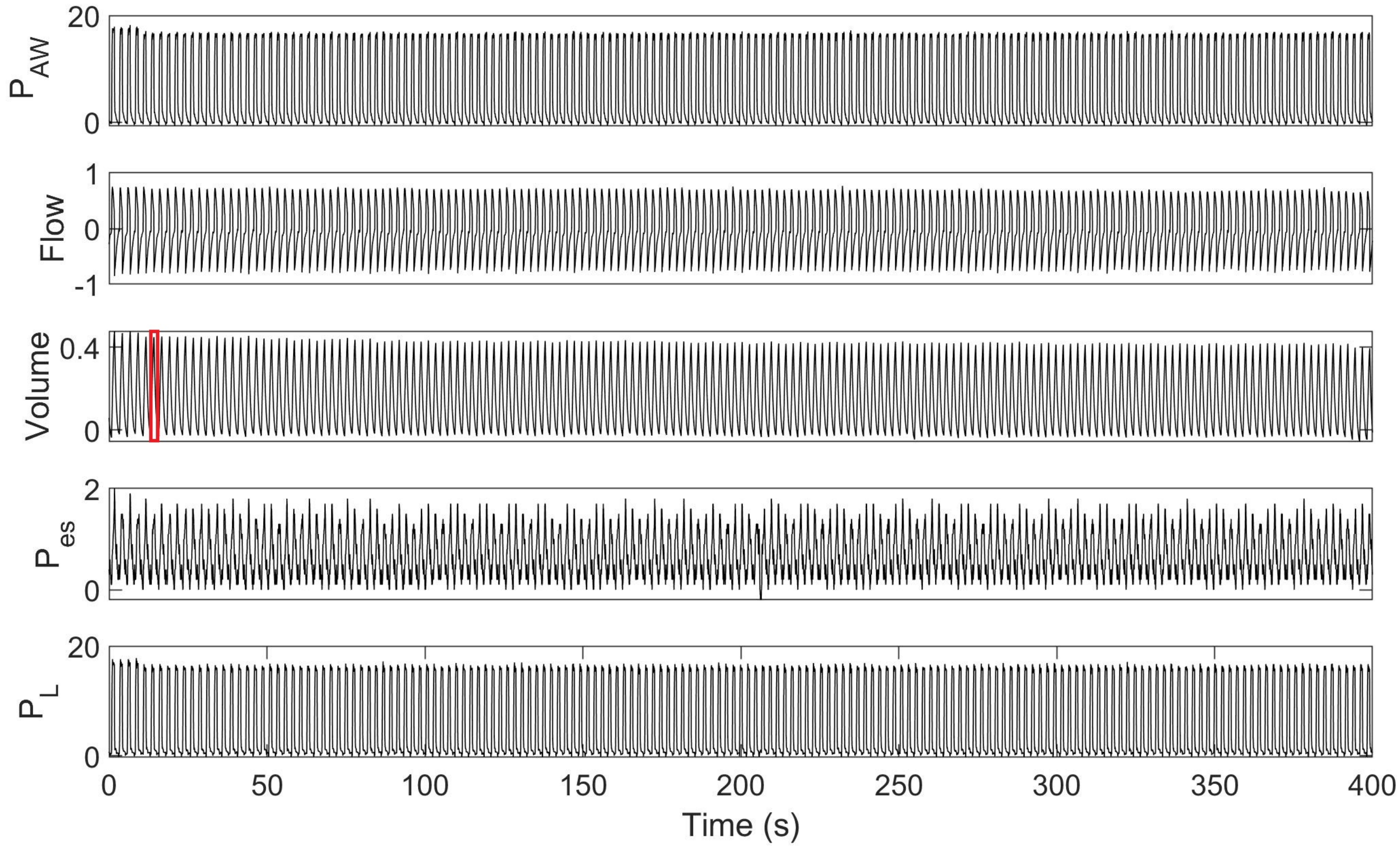

Preprocessed data of patient 5 used for system identification. The red box is the data frame used for system identification with the step experiment. P_{AW} is airway pressure, P_{es} is oesophageal pressure and P_L is transpulmonary pressure. P_{AW}, P_{es} and P_L are in cm H_2O. Volume is in L and flow in L s^{-1}.

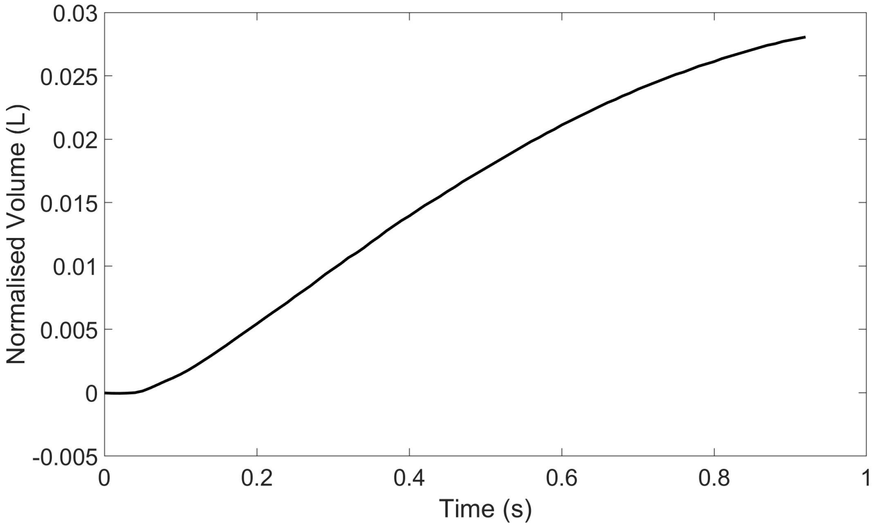

Single inspiratory leg of a breath used for system identification using the step experiment. The volume curve is normalised by dividing the signal with the pressure difference of airway pressure.

APPENDIX C: INSTRUCTION MANUAL MATLAB SCRIPTS: SYSTEM IDENTIFICATION

All MATLAB files can be found on: https://github.com/Amne96/Lung-Model.git

Patient data files are included in the MATLAB files for system identification. Both raw data and preprocessed data for system identification described in Appendix B are included in the patient files.

ELABORATION OF MATLAB SCRIPTS

- Main.m: the main file for system identification. Patient data files are loaded and the system identification algorithm (Sys_Iden.m) is run.
- Sys_Iden.m: function which runs all the different system identification methods described in this thesis. Function splits data files in train and validation data.
- Step_est.m: function for system identification using the step experiment. Function returns calculated parameters E and R with corresponding MSE of identified system.
- Step_opt.m: optimisation of system identification using the step experiment. The function returns the calculated E and R of the system with the smallest MSE.
- Blackbox.m: system identification of state space model, where the respiratory system is considered a black box. This allows for state matrices to be estimated without estimation value boundaries. This estimation leads to not physiological values for E and R. Function returns identified system, fit percentage, MSE, estimated parameter values and SE of estimated parameters.
- Grey_est.m: system identification of state space model, where the respiratory system is considered a grey box with parameters E and R to be estimated. These parameters are limited to a physiological range. Functions returns three identified models: respiratory system, lung and thorax. Each model contains identified system, fit-percentage, MSE, estimated parameter values and SE of estimated parameters. The model is identified with training data. Fit percentage, MSE and SE are determined with validation data.
- TF_est.m: system identification with a transfer function for the respiratory system. Function returns fit-percentage, MSE, estimated parameter values and standard error of estimated parameters. Estimation with transfer function or state space design are the same since both use the same optimisation algorithm. The model is identified with training data. Fit percentage, MSE and SE are determined with validation data.

APPENDIX D: INTERPOLATION OF EXPIRATORY LEG OF A BREATH

Due to air leak, expiratory volume is smaller than inspiratory volume. The ventilator resets the volume to zero for each new breath. This causes a large drop between the last sample of the first breath and the first sample of the breath after. The end of the expiratory phase can therefore be easily detected by taking the absolute value of the differential of the volume.

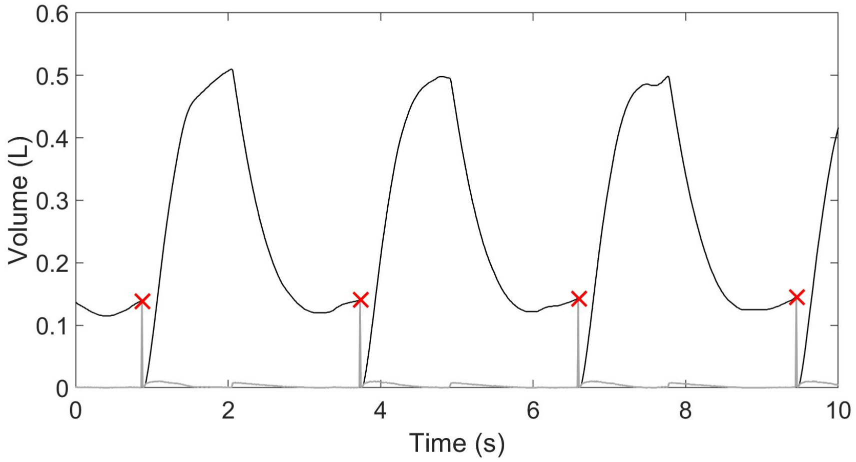

Interpolation of volume curve (black) of patient 1 where expiratory volume is smaller than inspiratory volume due to air leakage. The end of the expiration is identified using the absolute value of the differential of the volume curve (grey). The data samples with a lower value than the identified point (red cross) will be replaced with the value of the identified point. This results in the interpolated signal.

All data points with a lower value than the identified point are replaced with the value of the identified point. Note that inspiratory volume becomes smaller because the first 100 ml are cut away. To correct the offset of the interpolated signal, the offset value is subtracted from the curve.

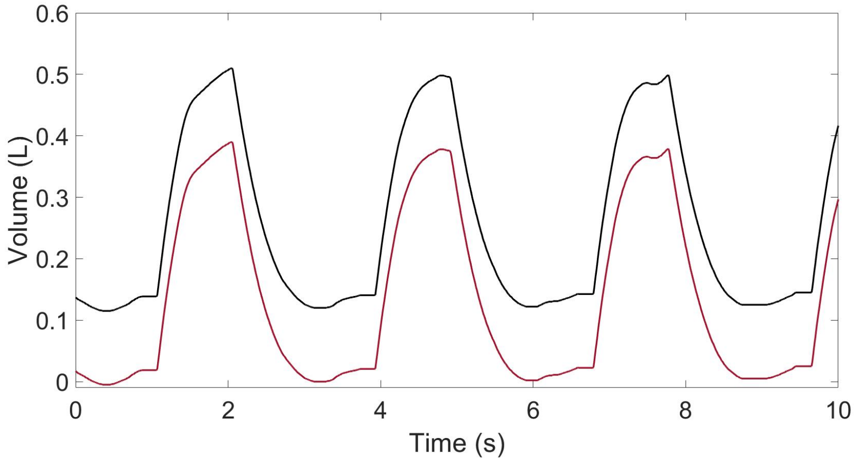

Result of volume curve after interpolation (black). The off set is subtracted (red) for system identification.

APPENDIX E: SIMULINK MODEL DESIGN

All MATLAB and Simulink files can be found on: https://github.com/Amne96/Lung-Model.git

Model.m contains all model parameters which should be run before running the simulation.

MECHANICAL VENTILATOR

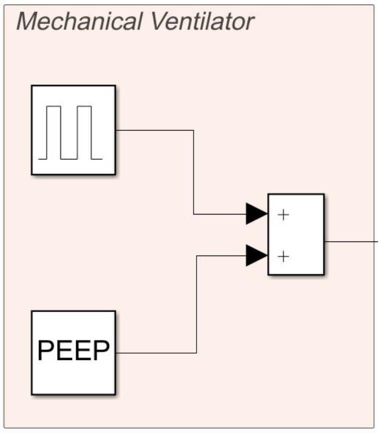
Mechanical Ventilator
+
+
PEEP

Simulink model of mechanical ventilator for pressure controlled mechanical ventilation. Positive end expiratory pressure (PEEP) is a constant. Inspiratory pressure waves are created with a pulse generator.

MODEL 1

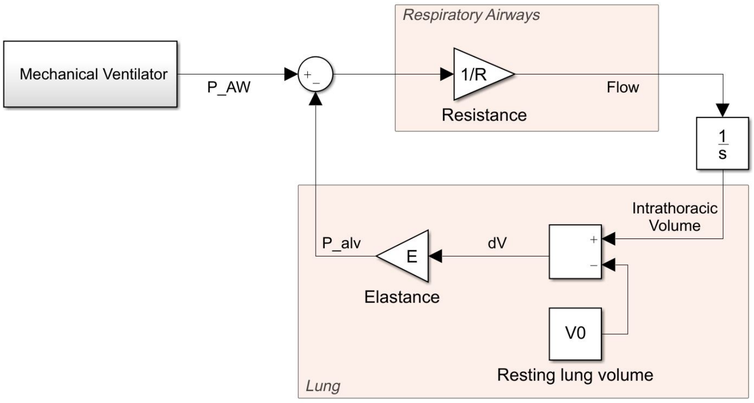
Mechanical Ventilator
P_AW
Respiratory Airways
1/R
Resistance
Flow
1
s
Intrathoracic
Volume
P_alv
E
Elastance
dV
V0
Resting lung volume
Lung

Model 1: Simulink model of first order linear model of the respiratory system. Elastance, resistance and resting volume are constants.

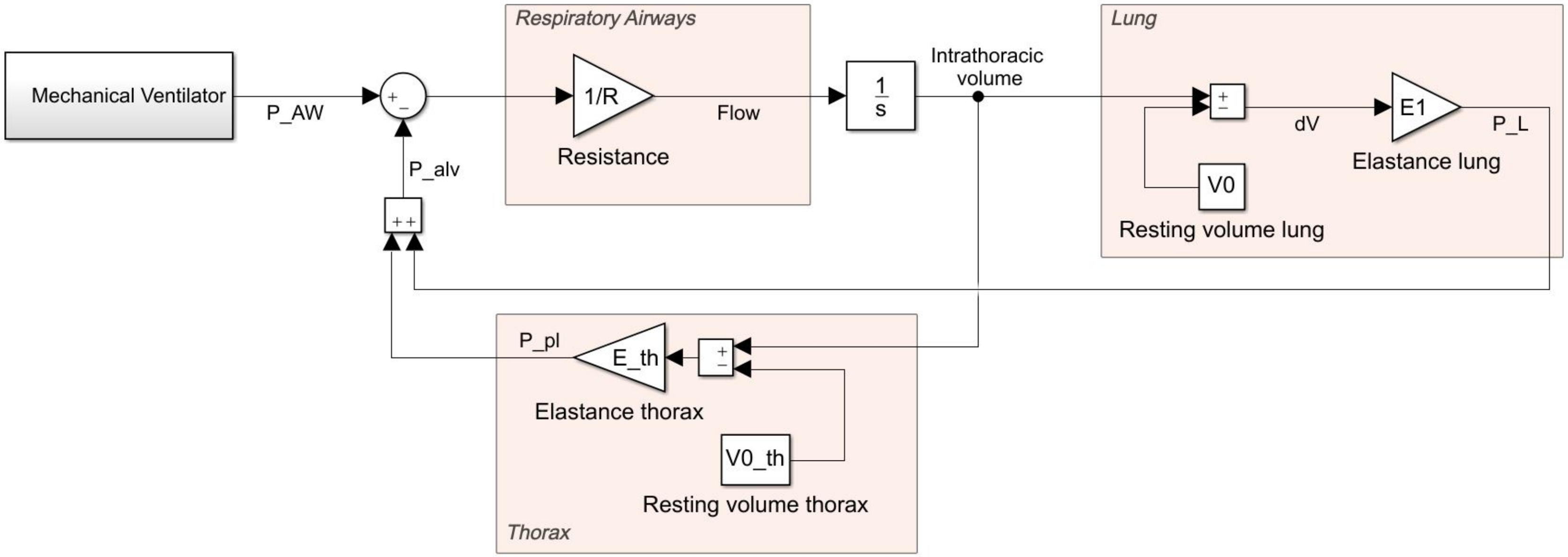
Mechanical Ventilator
P_AW
+
−
P_alv
+ +
Respiratory Airways
1/R
Resistance
Flow
1
s
Intrathoracic volume
Lung
+
−
dV
E1
P_L
Elastance lung
V0
Resting volume lung
P_pl
E_th
+
−
Elastance thorax
V0_th
Resting volume thorax
Thorax

Model 2: Simulink model of first order linear model of the respiratory system where the total elastance is made up from the lung elastance and thorax elastance. This results in separate calculation of transpulmonary pressure and pleural pressure. Elastances, resistance and resting volumes are constants.

MODEL 3

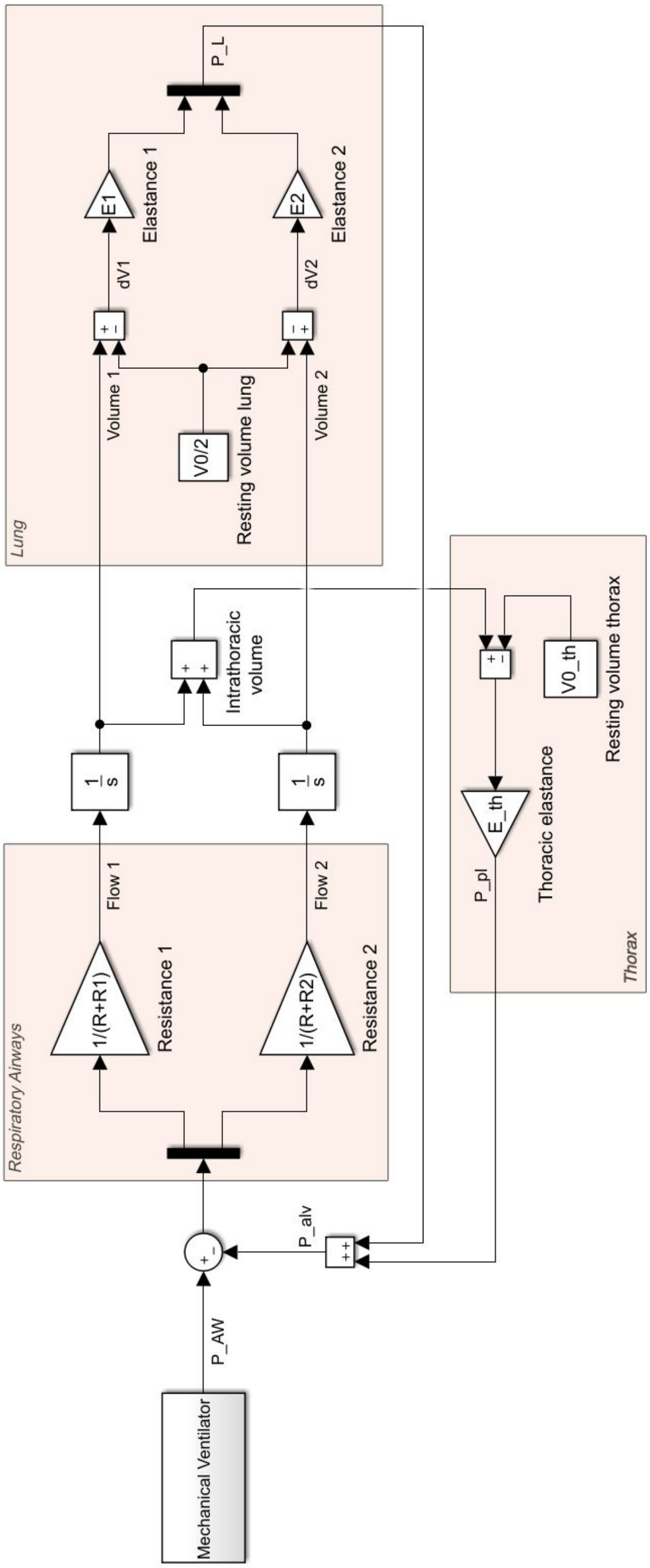
Mechanical Ventilator
P_AW
+
−
P_alv
+
+
Respiratory Airways
1/(R+R1)
Resistance 1
1/(R+R2)
Resistance 2
Flow 1
Flow 2
1/s
1/s
Intrathoracic volume
+
+
Lung
Volume 1
Volume 2
V0/2
Resting volume lung
+
−
−
+
dV1
dV2
E1
Elastance 1
E2
Elastance 2
P_L
Thorax
+
−
V0_th
Resting volume thorax
E_th
Thoracic elastance
P_pl

Model 3: Simulink model of first order linear model of the lung and thorax as separate components. The lung compartment is split in to two compartments which allows for simulation of heterogeneity of the lung. Parameter R represents the common resistance. Parameters R1, R2, E1 and E2 represent the elastance and resistance of the two lung compartments. Elastances, resistances and resting volumes are constants.

MODEL 4

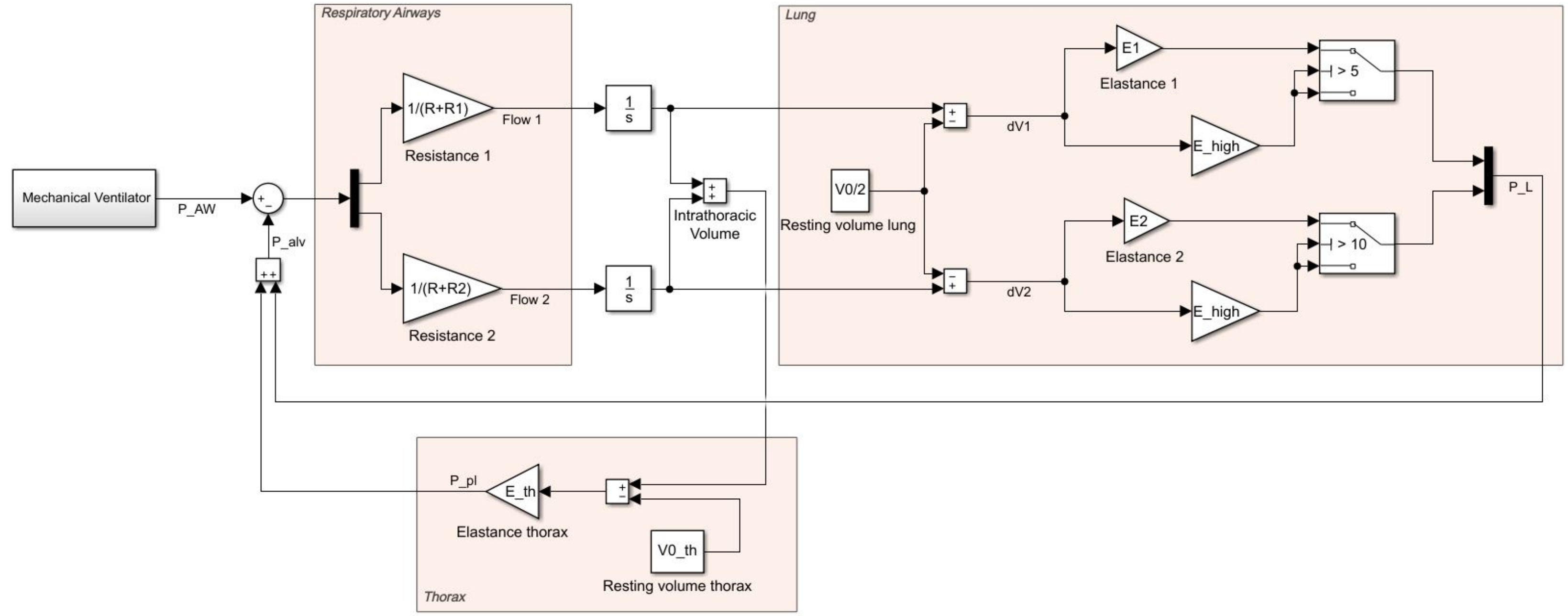
Mechanical Ventilator
P_AW
P_alv
Respiratory Airways
1/(R+R1)
Flow 1
Resistance 1
1/(R+R2)
Flow 2
Resistance 2
1
s
1
s
Intrathoracic
Volume
Lung
V0/2
Resting volume lung
dV1
dV2
E1
Elastance 1
E_high
> 5
E2
Elastance 2
E_high
> 10
P_L
Thorax
P_pl
E_th
Elastance thorax
V0_th
Resting volume thorax

Model 4: Simulink model of first order linear model of the lung and thorax as separate components. The lung compartment is split in to two compartments. Each compartment has its own threshold opening pressure (TOP) to simulate recruitment. Derecruitment is simulated with a very high elastance which does not allow inflation of that compartment. By increasing the alveolar pressure, the transpulmonary pressure increases until the TOP is reached. The system then 'flips' the switch to the low elastance; the compartment is recruited. TOP, elastances, resistances and resting volumes are constants. In this figure TOPs are 5 cm H_2O and 10 cm H_2O.